EUROPEAN ORGANIZATION FOR NUCLEAR RESEARCH
European Laboratory for Particle Physics

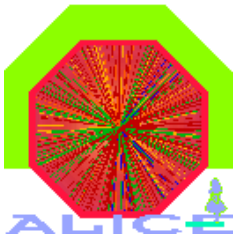

Internal Note/
ALICE reference number
ALICE-INT-2005-026 version 1.0
Institute reference number
[-]
Date of last change
19th July 2005

One and Two particle resolutions and PID. Results from PDC04 phase 1.

Authors:

Piotr Krzysztof Skowroński
Jan Pluta
Grzegorz Galązka
Michal Olędzki
Emilia Lubańska

Abstract:

We present the one and two particle resolutions obtained for the most central events produced during ALICE Physics Data Challenge 2004 (PDC04). This note intends to serve as a reference in the matters of the resolution and PID, documenting the status at the time of PDC04. The main accents are on the two particle problems. However, since deep understanding of the two particle effects requires knowledge of the the one particle ones, we also present here these results.
The note is organized as follows. In the introduction we briefly discuss all the potential effects leading to the biases in the measured two particle spectra. Afterwards, the simulation and reconstruction setup is shortly described. In the next two sections summary tables and plots are shown and discussed, observed anomalies are pointed out. Further, the obtained Particle Identification (PID) efficiency is presented. In the extensive appendixes we present all the detailed resolution plots.

Contents

1 Introduction

It is very important to control the distributions of the residuals. They define the resolution of the detector but also shows the eventual systematic shifts. From the detailed plots constructed with sufficiently high statistics one can learn about the performance of the reconstruction code.

We have analyzed the most central data produced during phase 1 of the Physics Data Challenge 2004 (PDC04). It was generated with the Hijing generator for the impact parameter range 0–2 fm that yields more then 6000 charged particles per unit of rapidity. Detailed description of the simulation and reconstruction software can be found at [1].

For each considered variable X we construct histograms of the difference between simulated and reconstructed values, further called ΔX. The order within difference is always kept so in case of any systematical shift the reader can distinguish if the reconstructed value is statistically under- or over-estimated. In the all cases the simulated value is plotted in horizontal axes.

We define resolution (also referred as RMS of ΔX) as a sigma of the Gaussian fit to a ΔX distribution. Whenever is plotted mean of ΔX it is the fitted expectation value.

In this analysis we consider only particles with correctly identified particle type (PID) and PID probability higher then 50%, unless stated explicitly otherwise. All the two particle distributions are made for pairs emitted (generated) with small momentum difference in the pair rest frame, namely $Q_{inv} < 50$ MeV/c. We analyze all two particle variables that are interesting for the interferometry in function of K_t and Q_{inv}, and sometimes a variable itself.

2 Definitions of the variables used in the close velocity correlations

The most important variable is the length of velocity difference vector $2k^*$. If particles have the same mass it is equivalent to the invariant momentum difference Q_{inv}. The vector can be decomposed to the following components, see Fig.1:

- *long* parallel to beam
- *side* perpendicular to beam and pair momentum K
- *out* perpendicular to *long* and *side*

The most adequate frame for the analysis is the so called Longitudinally CoMoving System (LCMS), where velocity components in beam (longitudinal) direction are equal. The LCMS frame is used through out this note.

Note also that for small opening angles the components *long* and *side* are approximately proportional to the relative polar (θ_{pair}) and azimuthal (ϕ_{pair}) angles, respectively. The *out* component is determined by the difference of the absolute values of transverse velocity and depends on the tracks curvature.

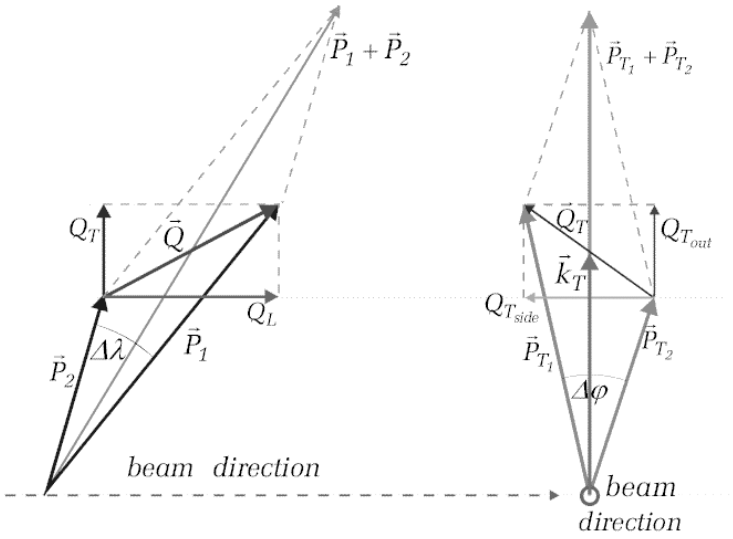

Figure 1: Basic kinematic variables of correlation analysis

3 Single particle resolutions

The very first important information is the resolution of the reconstructed p_t (transverse momentum), θ (polar angle) and ϕ (azimuthal angle), because these variables are independent parameters reconstructed by the tracking procedure.

The obtained distributions of the residuals for pions, kaons and protons are shown in Appendix A . We observe a non-negligible systematic shifts of transverse momentum residuals. The effect was explained as the (undocumented) feature of the reconstruction software that assumes the mass of electron while calculating the corrections for dEdX. The mass assumption is done after the very first reconstruction pass in TPC. At this point particle type can be determined only on the basis of dEdX in TPC. And indeed, the systematic shift occurs mostly for the transverse momentum ranges at which dEdX overlaps with electrons for a given particle type, see Fig.2. The actual problem was the lack of the final refit in the reconstruction chain using the most probable mass, when all the information is available. In the consequence a particle is reconstructed with the correct PID and tracked like an electron. The observation was communicated to the tracking developers and appropriate corrections were applied.

The systematic skew is relatively small for pions, and as it can be learned from the following section, it has a negligible influence on the two particle properties. However, the effect exhibits itself for the two particle systems that involve kaons or protons (it is discussed in the next section).

The pion transverse momentum resolution (Fig.11a) is of the order of 0.7% while the value estimated in Alice Technical Proposal [2] is around 1.3%. Taking into account the fact that the results presented in TP were calculated with the magnetic field 0.2 T, while

here 0.5 T is used, the results are compatible. The p_t resolutions for kaons and protons are also close to the prediction. Similarly all angular resolutions for all the considered particle types are in the good agreement with TP.

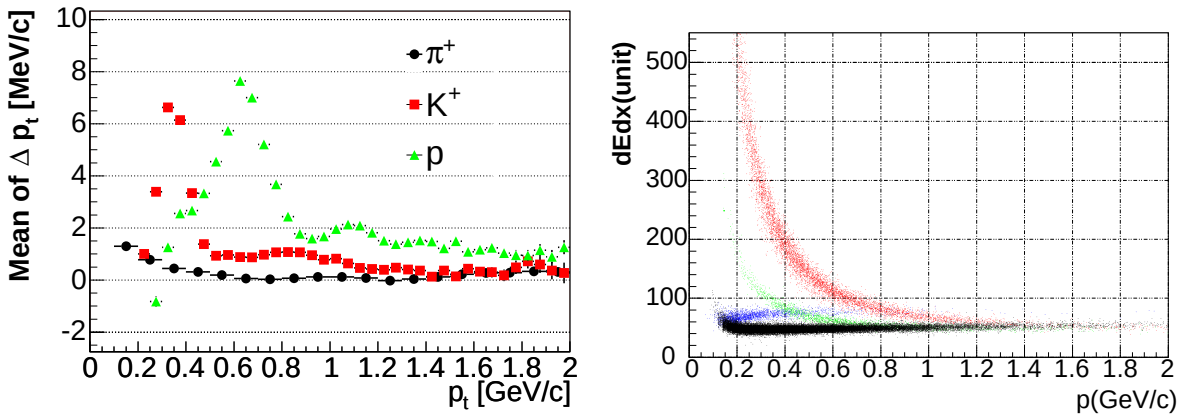

(a) (b)

Figure 2: a) Mean of p_t residuals versus p_t and b) dE/dX versus momentum in TPC.

4 Two particle resolutions

4.1 Identical particle systems

Before we move to the HBT variables, we perform the check of the simplest two particle ones: the angles between particles. For each system residuals of polar (θ_{pair}) and azimuthal (ϕ_{pair}) open angles as function of K_t and Q_{inv} are constructed. We have checked that there are no systematic skews i.e. the mean vales are consistent with zero within statistical errors.

$p_t$range [MeV/c]	Resolution (r.m.s) [MeV/c]			
	Q_{inv}	Q_{out}	Q_{side}	Q_{long}
$100 < p_t < 300$	0.95	2.70	0.34	0.95
$300 < p_t < 600$	0.99	3.62	0.40	1.12
$600 < p_t$	1.17	6.33	0.62	1.42

Table 1: Resolutions of the HBT variables for $\pi^+\pi^+$ system.

Resolutions of Q_{inv}, Q_{side}, Q_{long} and Q_{out} versus K_t and Q_{inv} are presented in Figures

3, 4 and 5 for pions, kaons and protons, respectively. Because resolution of Q_{out} increases strongly with K_t, we decided not to put it in the same plot with the other components. They can be found in Fig.21 (pions), Fig.4 (kaons) and Fig.41 (protons). The numerical values for pions are summarized in Table 1 so they can be compared with Table 11.6 of TP. The obtained results are very close. The discrepancies mainly result from the different magnetic field used in the simulations (better transverse momentum resolutions).

Only Q_{out} resolution sightly improves for very small values of Q_{inv}, while the other components do not depend on Q_{inv}, i.e. the proximity of another track does not deplete statistically the precision of the measurement. Almost all variables bears some systematic skews. However, in most of the cases they are much smaller then 1 MeV and they can be neglected.

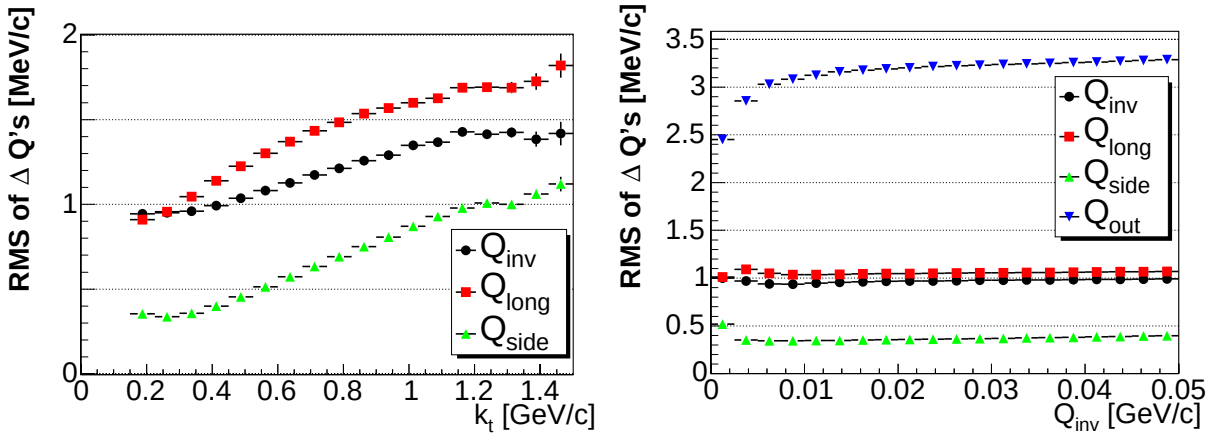

(a) (b)

Figure 3: $\pi^+\pi^+$ resolutions of Q_{inv}, Q_{side}, Q_{long} and Q_{out} versus a) K_t and b) Q_{inv}. Q_{out} resolution as function of K_t is presented in Fig.21

4.2 Non-identical particle systems

The obtained resolutions of $2k^\star$ for different systems are listed in Table 2, which can be compared with Table 11.7 in TP. The systematic skews are present basically for all of the considered systems. In all the cases the *out* component is the most affected (not shown), what is the result of the effect in transverse momenta. Since the p_t systematic shifts are the biggest for kaons and protons, systems invlolving these particles are the most affected and the biggest effect is observed for kaon-proton correlations.

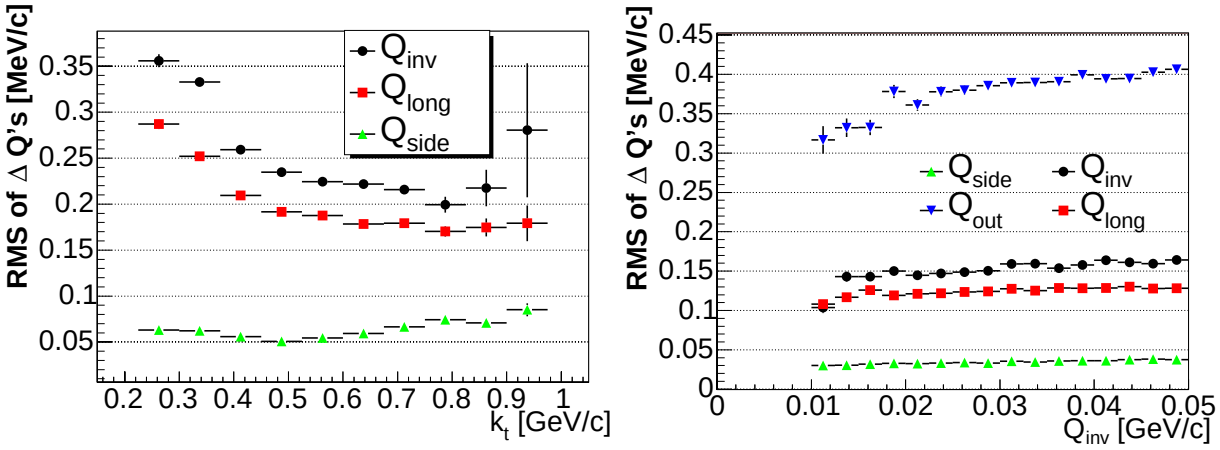

(a) (b)

Figure 4: K^+K^+ resolutions of Q_{inv}, Q_{side}, Q_{long} and Q_{out} versus a) K_t and b) Q_{inv}. Q_{out} resolution as function of K_t is presented in Fig.30

Particle system	$2k^\star$ [MeV/c]
$\pi^+\pi^-$	1.0
π^+K^+	1.4
π^+K^-	1.4
π^+p	1.7
$\pi^+\bar{p}$	1.7
K^+K^-	2.6
K^+p	3.6
$K^+\bar{p}$	3.4
K^-p	3.5
$K^-\bar{p}$	3.4

Table 2: $2k^\star$ resolutions for different particle systems

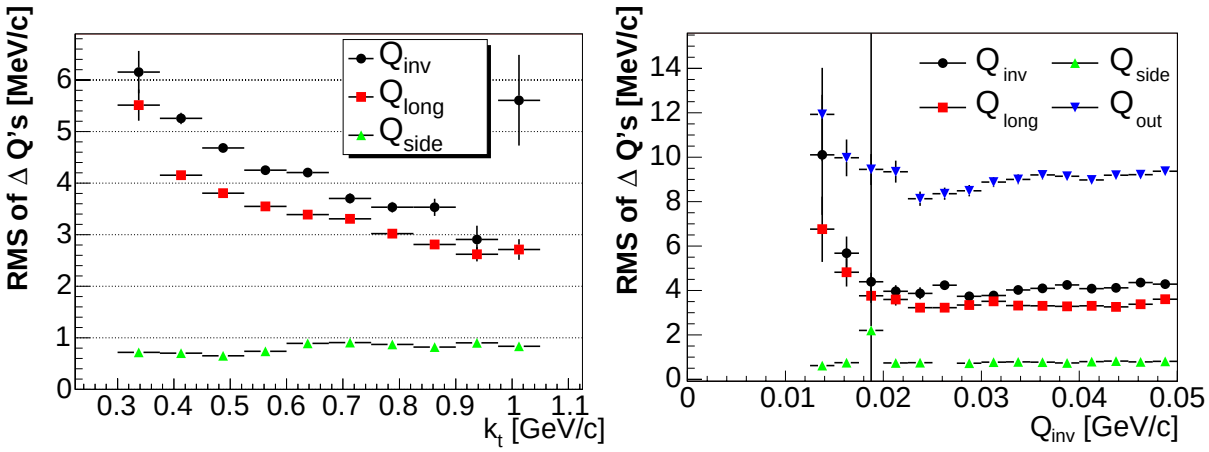

(a) (b)

Figure 5: *proton* − *proton* resolutions of Q_{inv}, Q_{side}, Q_{long} versus a) K_t and b) Q_{inv}. Q_{out} resolution as function of K_t is presented in Fig.41

5 Particle Identification

5.1 Single Particle PID

5.1.1 Pions

In figure Fig.6a we present pion contaminations versus p_t for different threshold values of the particle identification probabilities. Contamination is below 5% in p_t range up to 700 MeV, even for such low probability threshold as 50%. For higher transverse momenta it is necessary to set it as high as 90% in order to obtain such a high efficiency. However, in this case almost 50% of correctly identified pions is rejected, what can be seen in Fig.6b. This figure presents *rejection factor* i.e. ratio of correctly identified pions to this number in the case the threshold value is set to 0, from which the reader can learn how much the pion statistics is reduced at given p_t.

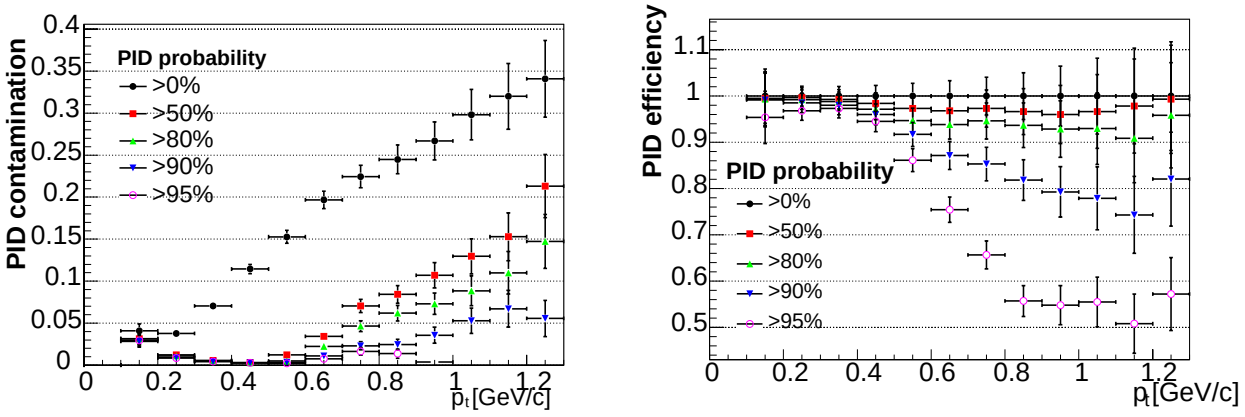

(a) (b)

Figure 6: a) PID contamination versus p_t for different probability threshold, and b) rejection factor for different probability thresholds in function of p_t for π^+

5.1.2 Kaons

The efficiency is very good at the lowest reconstructible transverse momenta. It worsens with p_t as the dE/dx of kaons and pions becomes comparable. Around 0.8 GeV the contamination reaches its maximum value of 25% and decreases for higher values as pions and kaons can be better distinguished by the time-of-flight.

One can see that the points for the threshold value of 0% and 50% are identical. As it can be learned from the Fig.7 the distribution sharply ends at 50% what indicates that there is an implicit cut in the reconstruction code. This is also true in case of protons.

From the comparison of the left and right plot in Fig.7 the reader can find out what is the penalty in statistics of the purity enhancement. At some p_t ranges it is more than 50% with the contamination reduction only about 3%.

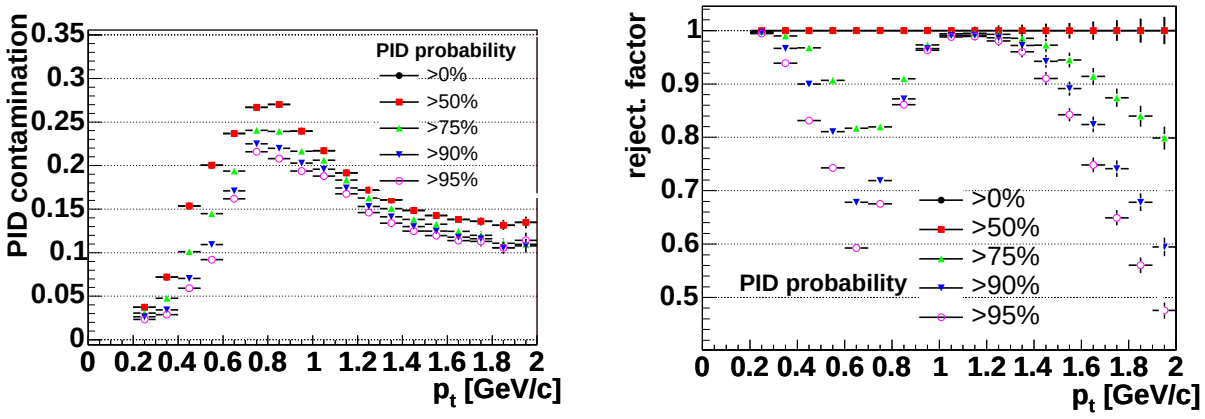

(a) (b)

Figure 7: a) PID contamination versus p_t for different probability threshold and b) rejection factor for different probability thresholds in function of p_t for kaons.

5.1.3 Protons

The PID efficiency for protons (Fig.8) is very high at the lowest reconstructible transverse momenta, because dEdX is much larger then for any other particle type what makes them easy to distinguish, see Fig.2b. With increasing p_t the efficiency decreases and reaches the smallest value (90-92%) at the range where proton dEdX is very similar to the pion one, i.e. 1.4–1.6 GeV. Afterwords the efficiency increases as pions and protons can be distinguished with the time-of-flight.

5.1.4 PID probability as the efficiency estimator

In the real data analysis the PID efficiency is unknown. Although in many cases it useful to have at least statistical control of the purity of a sample. The distribution of PID probability usually serves as such a tool. In Fig. 9b the distributions of the average PID probability and efficiency as function of transverse momentum for kaons are compared. We show here the example for which the discrepancy is the worst, although it is clear that the tuning of the PID reconstruction code is necessary in order to use the former one as the estimator of the latter one.

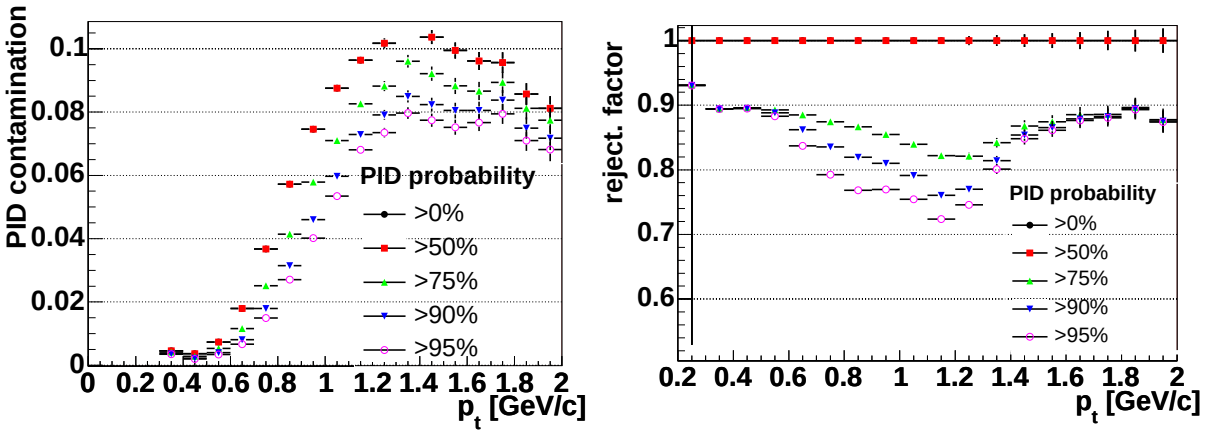

(a) (b)

Figure 8: a) PID contamination versus p_t for different probability thresholds and b) rejection factor for different probability thresholds in function of p_t for protons.

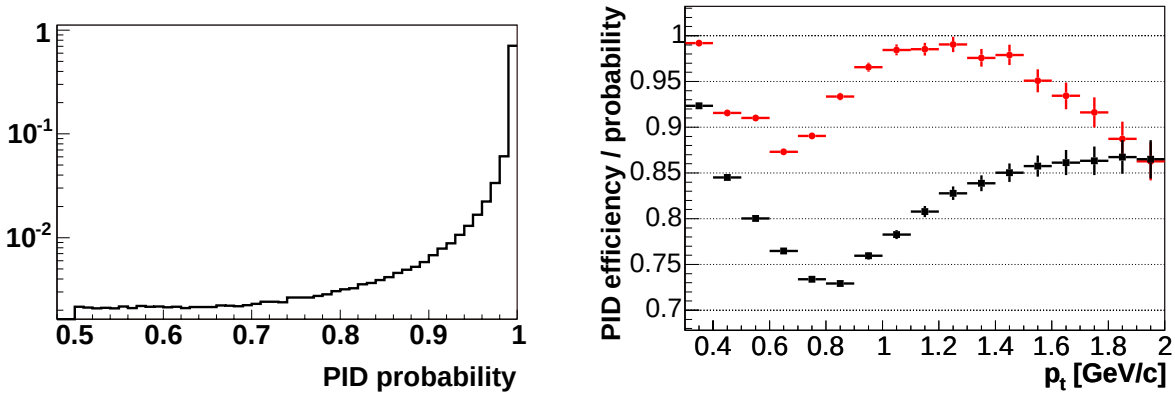

(a) (b)

Figure 9: a) Distribution of PID probability for protons. b) Average kaon PID probability (black squares) and efficiency (red circles) as function of p_t

5.2 Two Particle PID

Quality of a Particle Identification (PID) can be also dependent on the proximity of other tracks. Clusters can be shared between two tracks decreasing this way the quality of dE/dX measurement, thus making PID recognition more difficult and less efficient. In such cases it is easier to swap signals corresponding to the neighboring track when matching signal between sub-detectors.

In the experimental data analysis the pair purity (ratio of the number of pairs with both particles correctly identified to the number of all pairs) can be estimated from the product of the particle PID probabilities, which is further referred as the *pair probability*. Although, already from the previous section it is clear that the reconstruction code was not yet tuned appropriately to do that, we compare here also these distributions.

In Figure 10 are shown pair purities and probabilities for $\pi^+\pi^+$, K^+K^+ and pp systems as function of Q_{out}, Q_{side} and Q_{long}. In all the cases the PID efficiency does not change with any of the Q variables. The very slight dependence on Q_{out} for pions results from the uneven contribution of particles different transverse momenta to each Q_{out} bin. The efficiency decreases as the contribution of pions with larger p_t increases, see Fig. 6a.

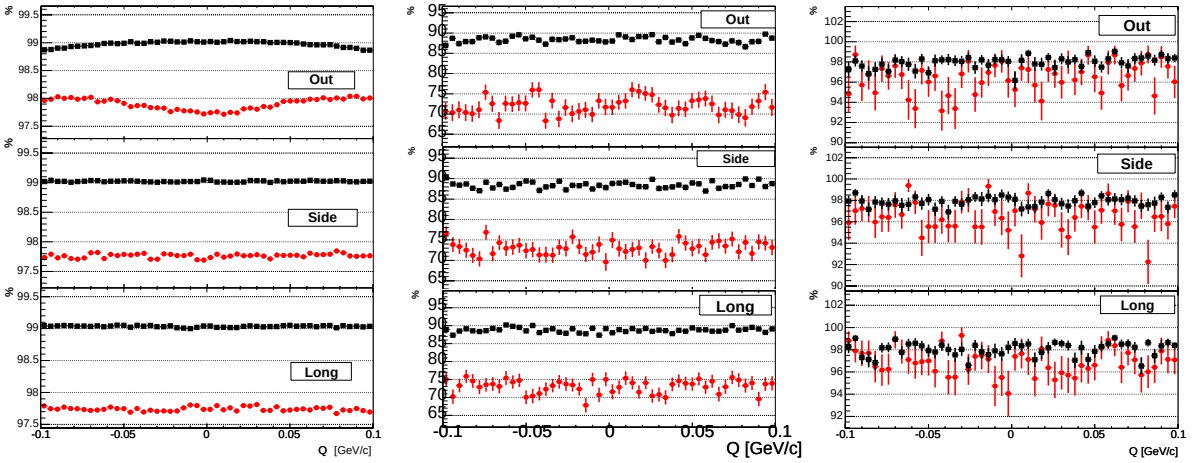

(a) (b) (c)

Figure 10: Pair probability (black squares) and efficiency (red circles) versus Q_{out}, Q_{side} and Q_{long} for a) $\pi^+\pi^+$ b) K^+K^+ and c) pp. The plots are constructed by projecting 3D histograms for the absolute values of the other coordinates < 20 MeV.

6 Summary and Conclusions

We have presented the resolution and PID efficiency obtained with the most detailed available simulation setup. The results show that the Alice detector performs very well, following the design requirements drawn in the Alice Technical Proposal. The direct comparison of these results is impossible because (in agreement with the current Alice baseline) the higher magnetic field was used in PDC04 simulations. However, it is clear that the obtained resolutions are better then the TP estimations .

We have pointed out the two problems in the reconstruction, namely

1. the systematic shifts in the reconstructed transverse momenta
2. the PID efficiency is far from coincide with the average PID probability for a given sample

Appendixes

A One particle resolutions

In the top plot of Fig.11a is shown the distribution of Δp_t. The middle and bottom plots shows RMS and Mean of the upper one. Appropriate plots for azimuthal angle ϕ and polar angle θ are shown in Fig.13 and Fig.16, respectively.

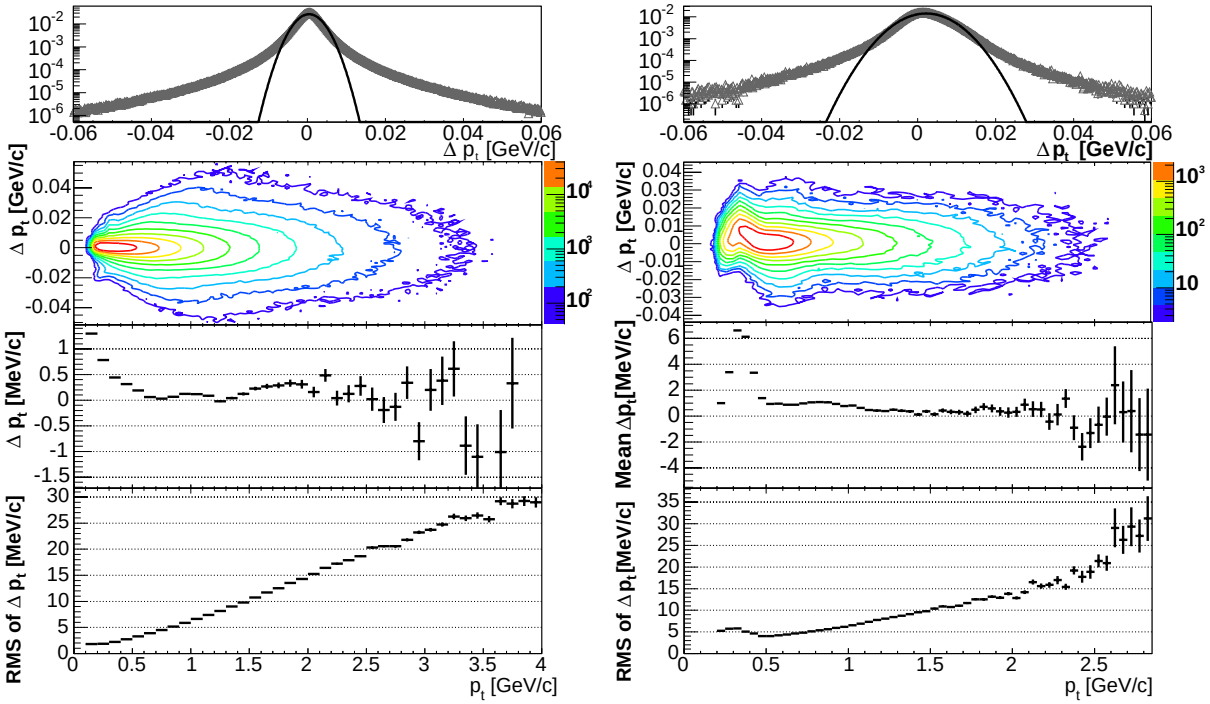

(a) (b)

Figure 11: p_t resolution versus p_t for (a) π^+ and (b) $K+$

Particle	Resolution		
	p_t[MeV/c]	θ [mrad]	ϕ [mrad]
π^+	1.9	2.3	2.9
K^+	0.7	1.9	5.4
p	2.0	2.4	7.7

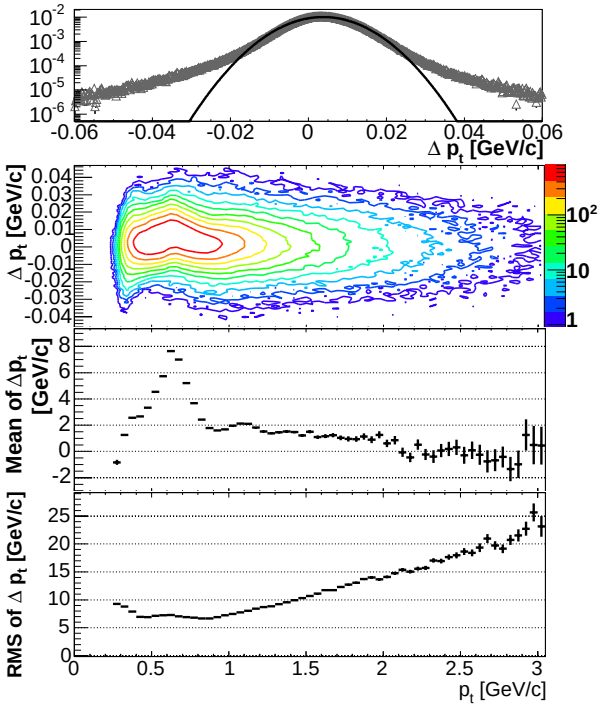

(a)

Figure 12: p_t resolution versus p_t for *proton*

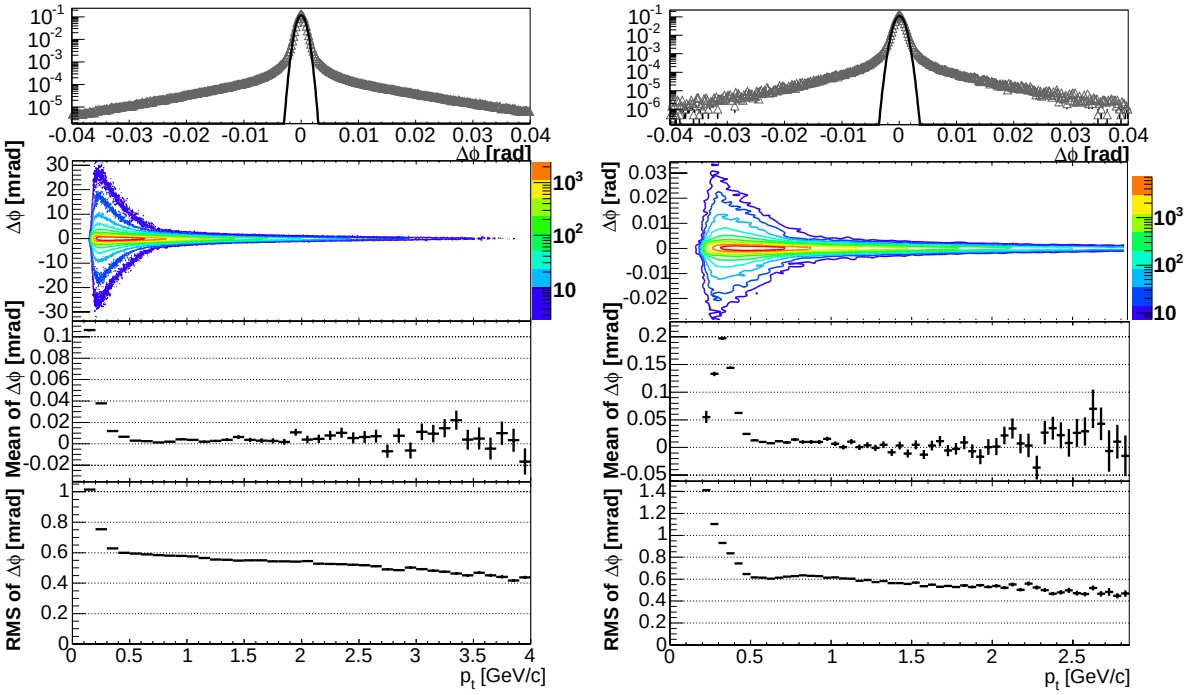

(a) (b)

Figure 13: ϕ resolution versus p_t for π^+ (a) and K^+ (b)

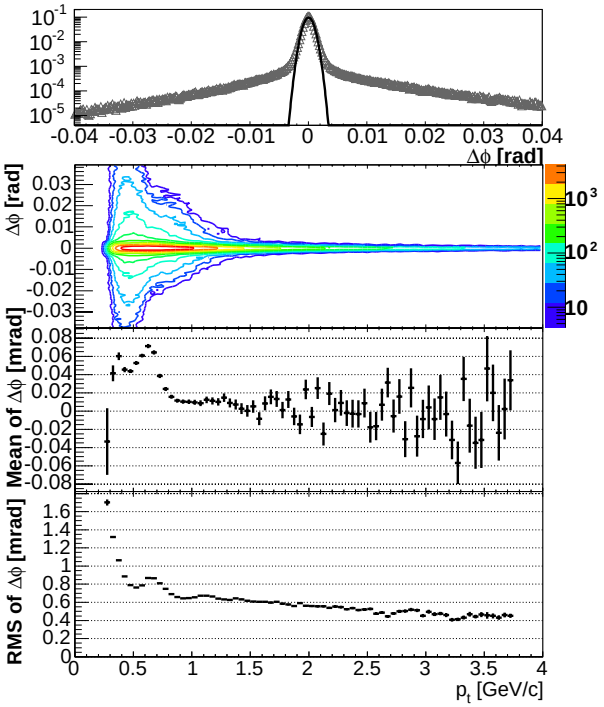

(a)

Figure 14: ϕ resolution versus p_t for *proton*

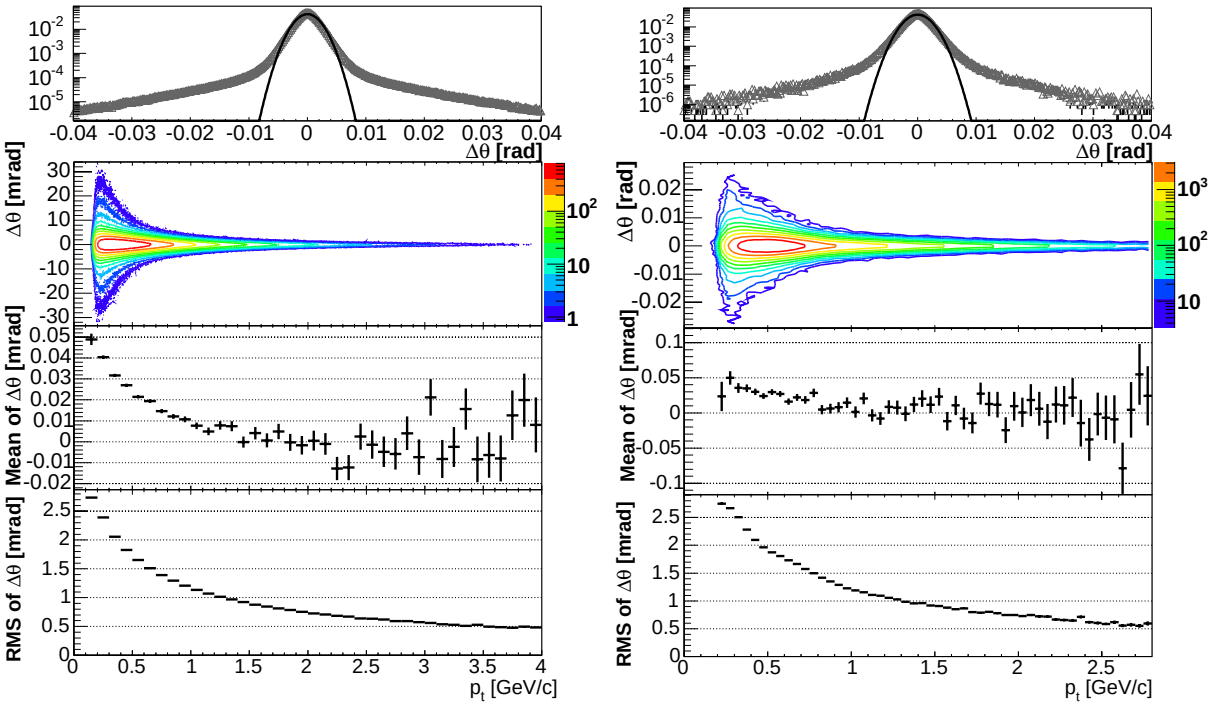

(a) (b)

Figure 15: θ resolution versus p_t for π^+ (a) and K^+ (b)

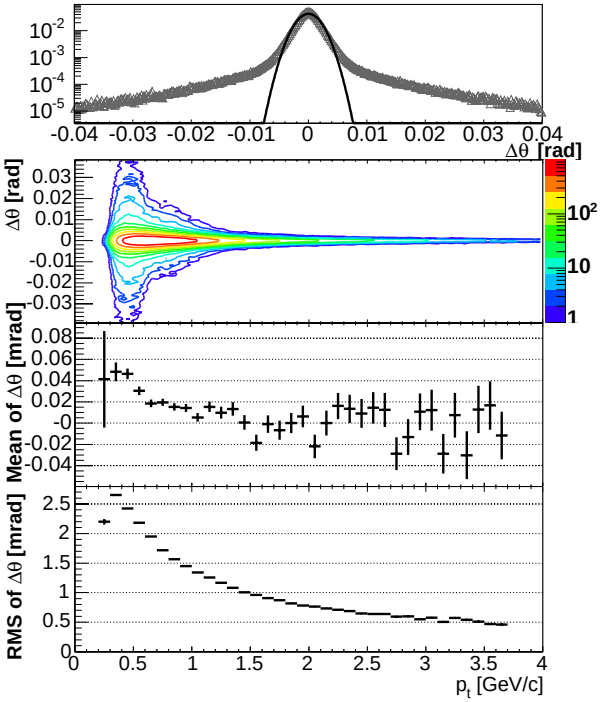

(a)

Figure 16: θ resolution versus p_t for *proton*

B Two particle resolutions

B.1 Identical

B.1.1 $\pi^+\pi^+$

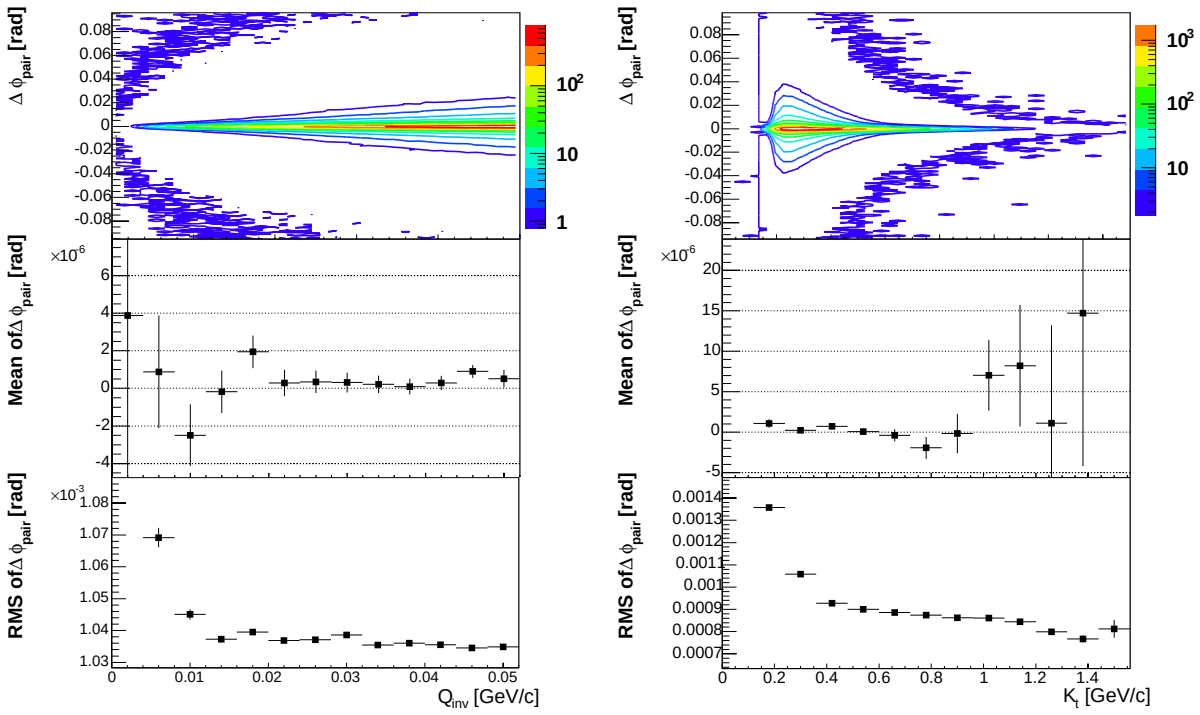

(a) (b)

Figure 17: ϕ_{pair} resolution versus a) Q_{inv} and b) K_t for $\pi^+\pi^+$ system.

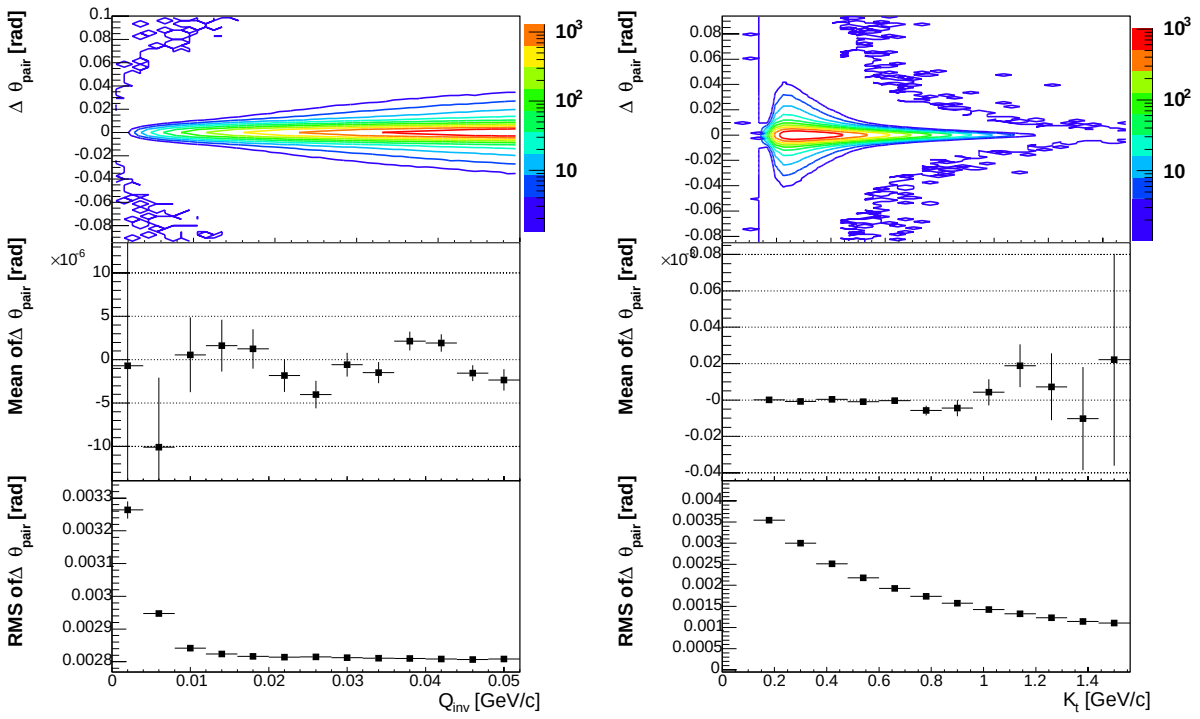

(a) (b)

Figure 18: θ_{pair} resolution versus a) Q_{inv} and b) K_t for $\pi^+\pi^+$ system

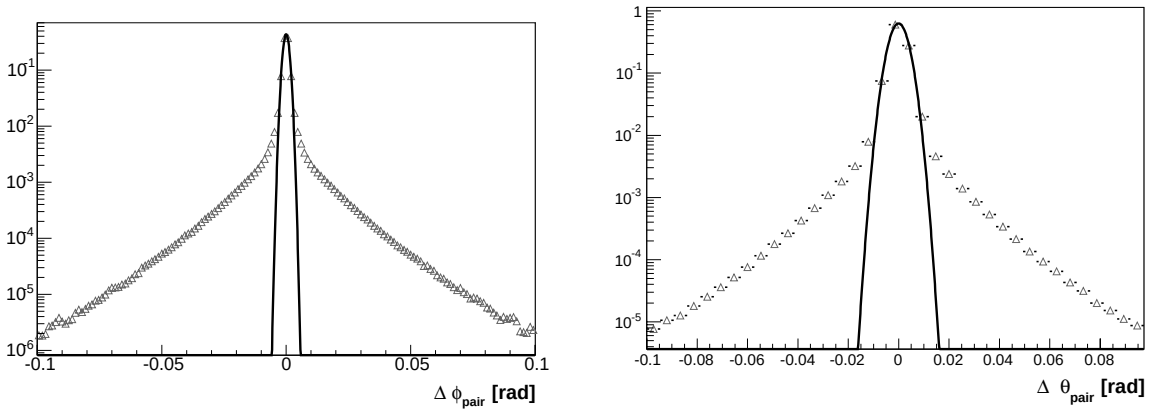

(a) (b)

Figure 19: Integrated residuals for ϕ_{pair} (1) and θ_{pair} for $\pi^+\pi^+$ system

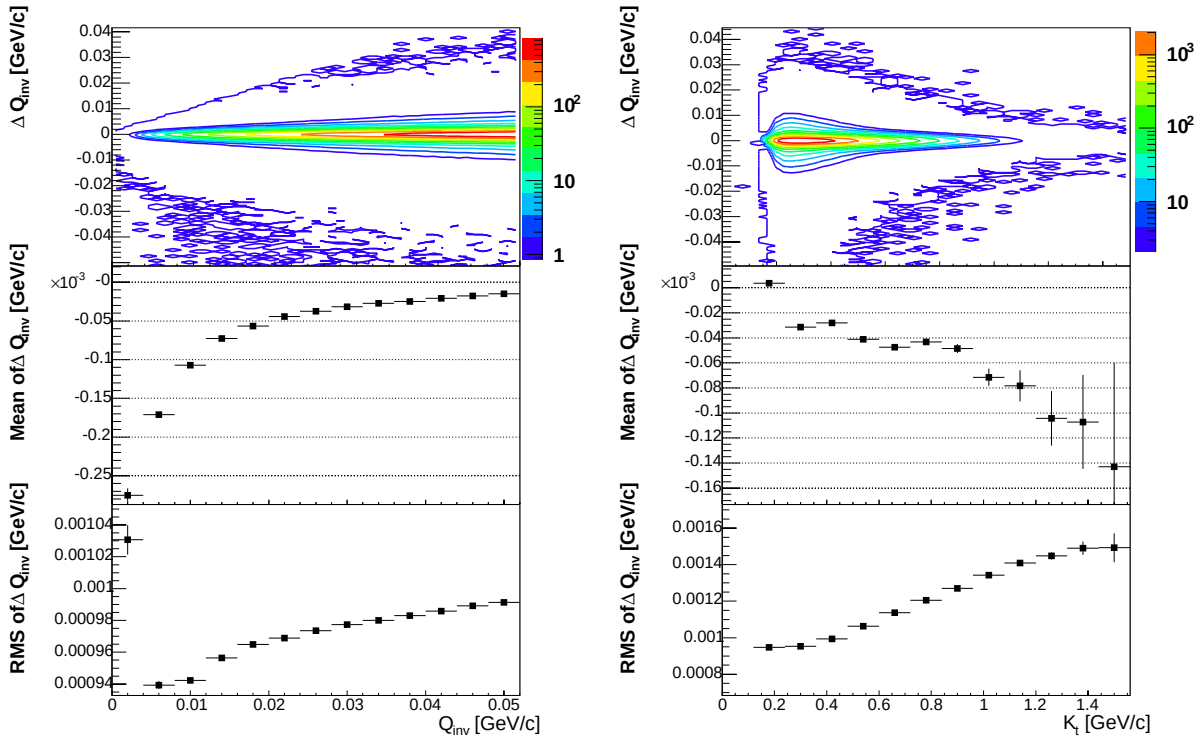

(a) (b)

Figure 20: Q_{inv} resolution versus (a) Q_{inv} and (b) K_t for $\pi^+\pi^+$ system

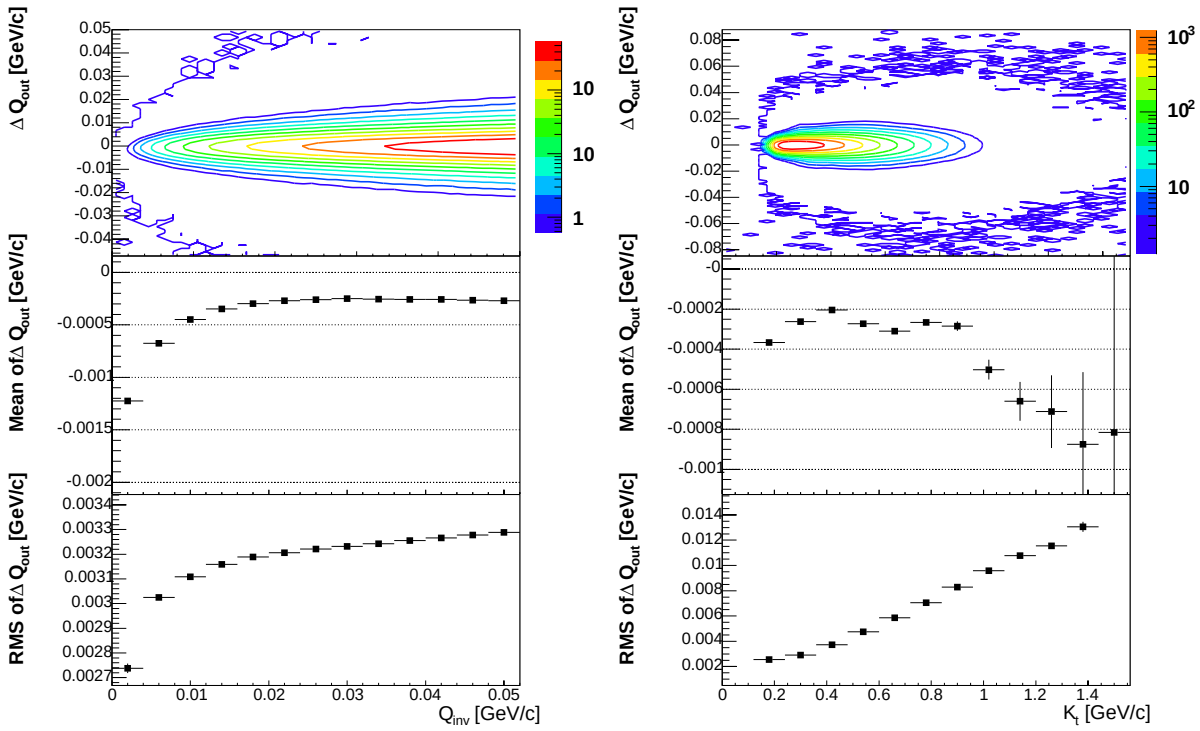

(a) (b)

Figure 21: Q_{out} resolution versus (a) Q_{inv} and (b) K_t for $\pi^+\pi^+$ system

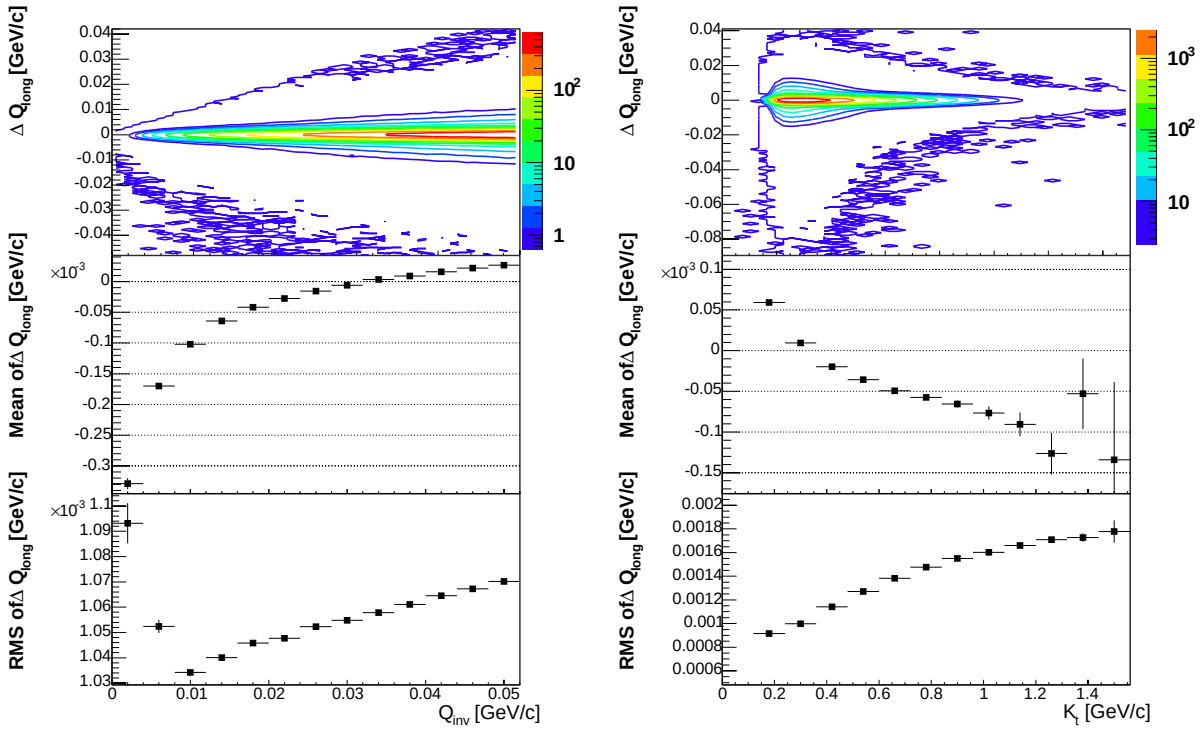

(a) (b)

Figure 22: Q_{long} resolution versus (a) Q_{inv} and (b) K_t for $\pi^+\pi^+$ system

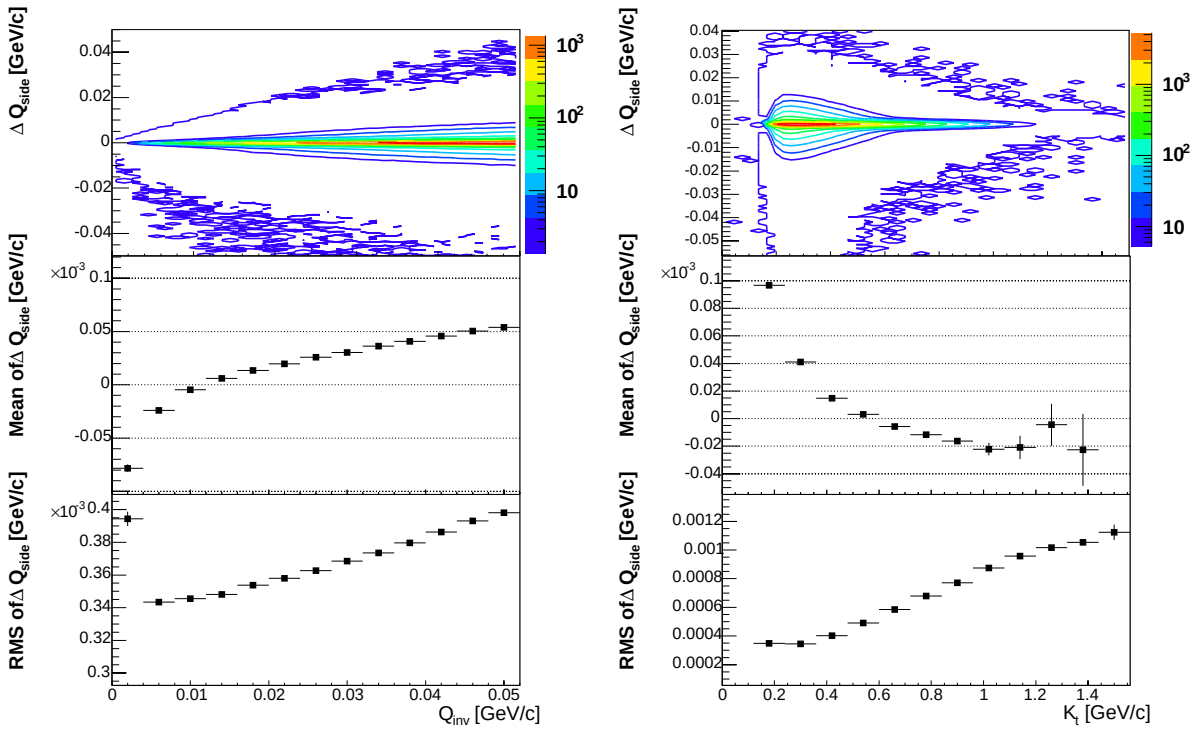

(a) (b)

Figure 23: Q_{side} resolution versus (a) Q_{inv} and (b) K_t for $\pi^+\pi^+$ system

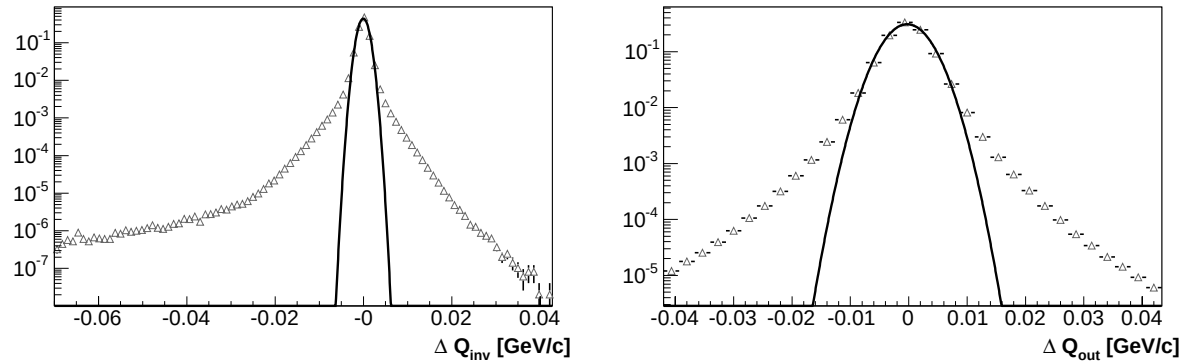

(a) (b)

Figure 24: Integrated residuals for (a) Q_{inv} and (b) Q_{out} for $\pi^+\pi^+$ system

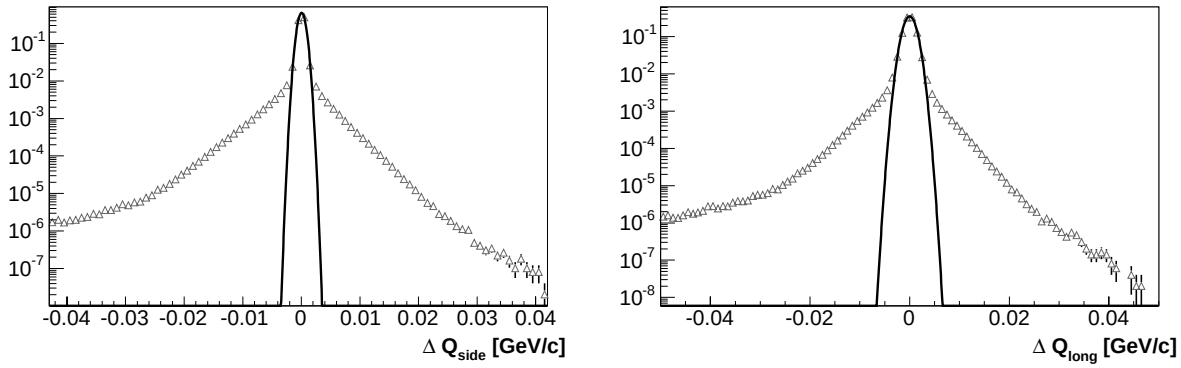

(a) (b)

Figure 25: Integrated residuals for (a) Q_{side} and (b) Q_{long} for $\pi^+\pi^+$ system

B.1.2 K^+K^+

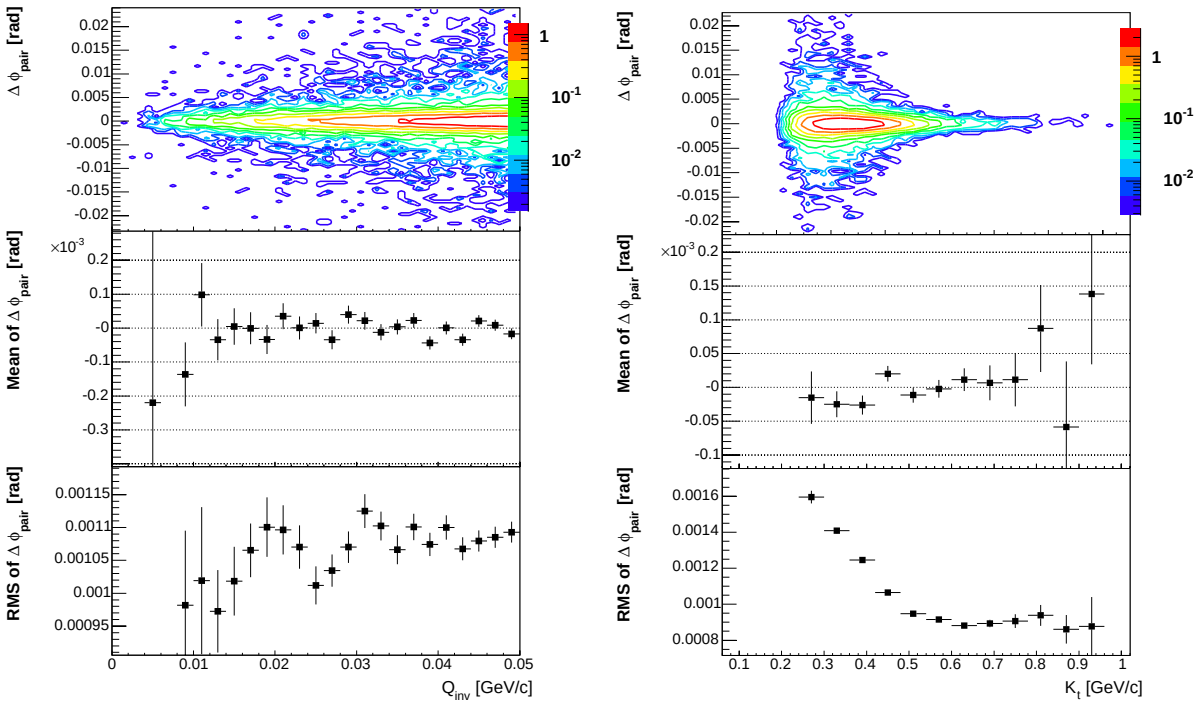

(a) (b)

Figure 26: ϕ_{pair} resolution versus Q_{inv} (a) and K_t (b) for K^+K^+ system.

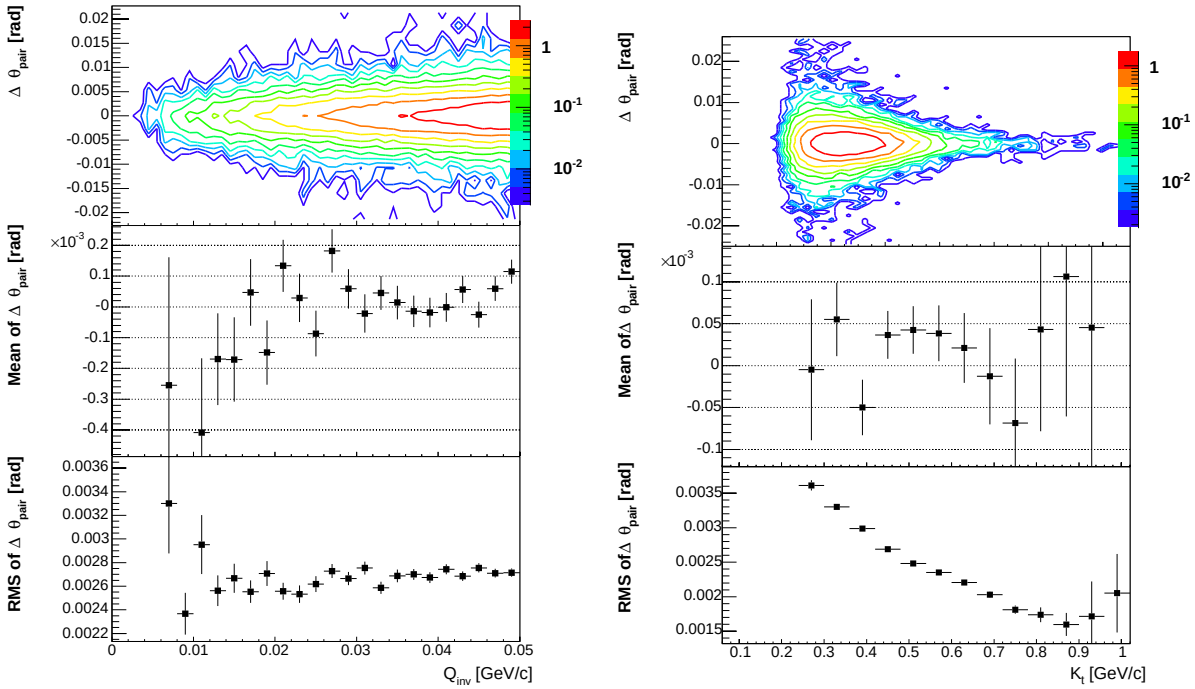

(a) (b)

Figure 27: θ_{pair} resolution versus Q_{inv} (a) and K_t (b) for K^+K^+ system

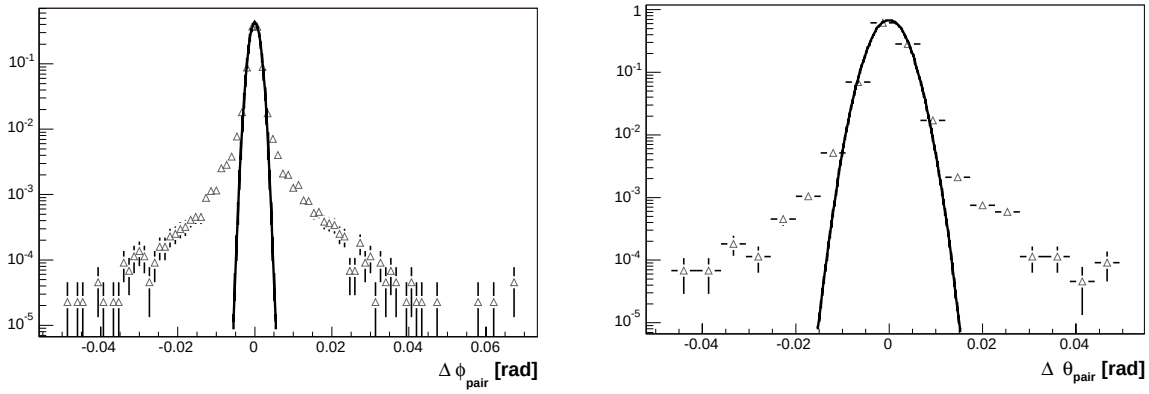

(a) (b)

Figure 28: Integrated residuals for ϕ_{pair} (a) and θ_{pair} (b) for K^+K^+ system

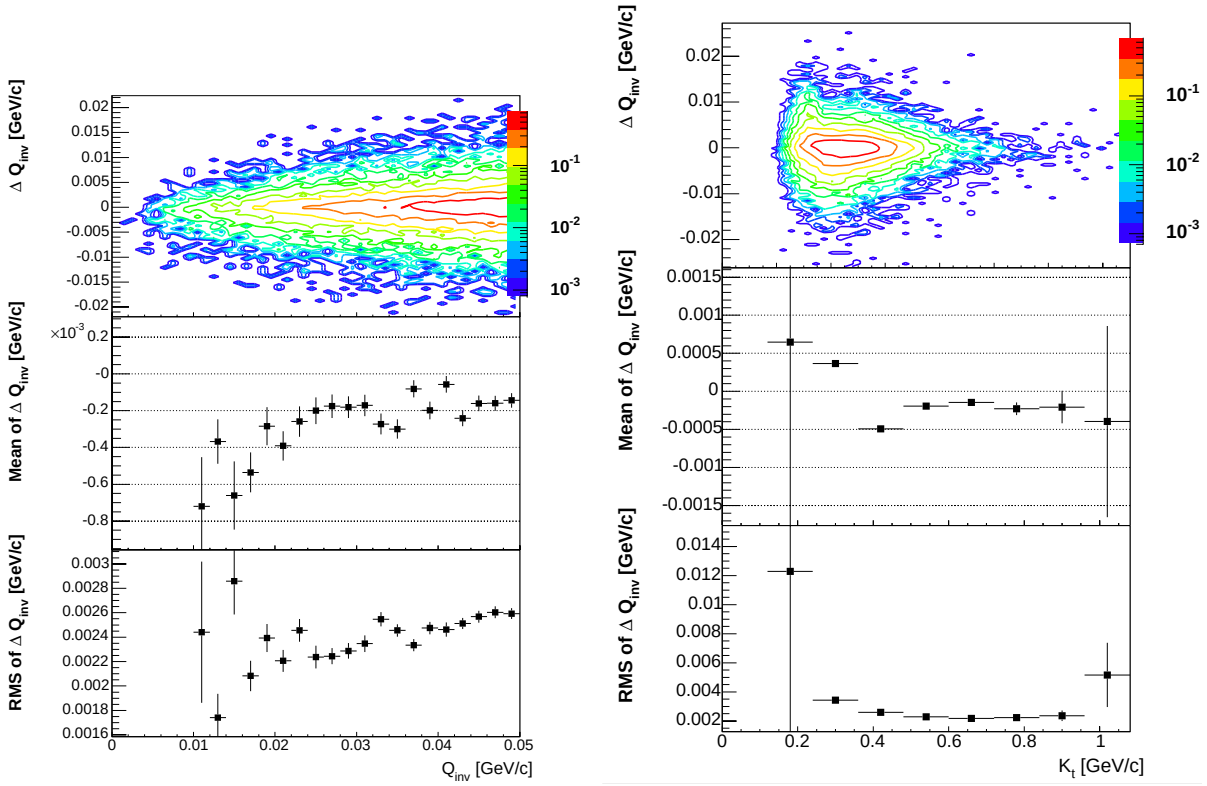

(a) (b)

Figure 29: Q_{inv} resolution versus Q_{inv} (a) and K_t for K^+K^+ system

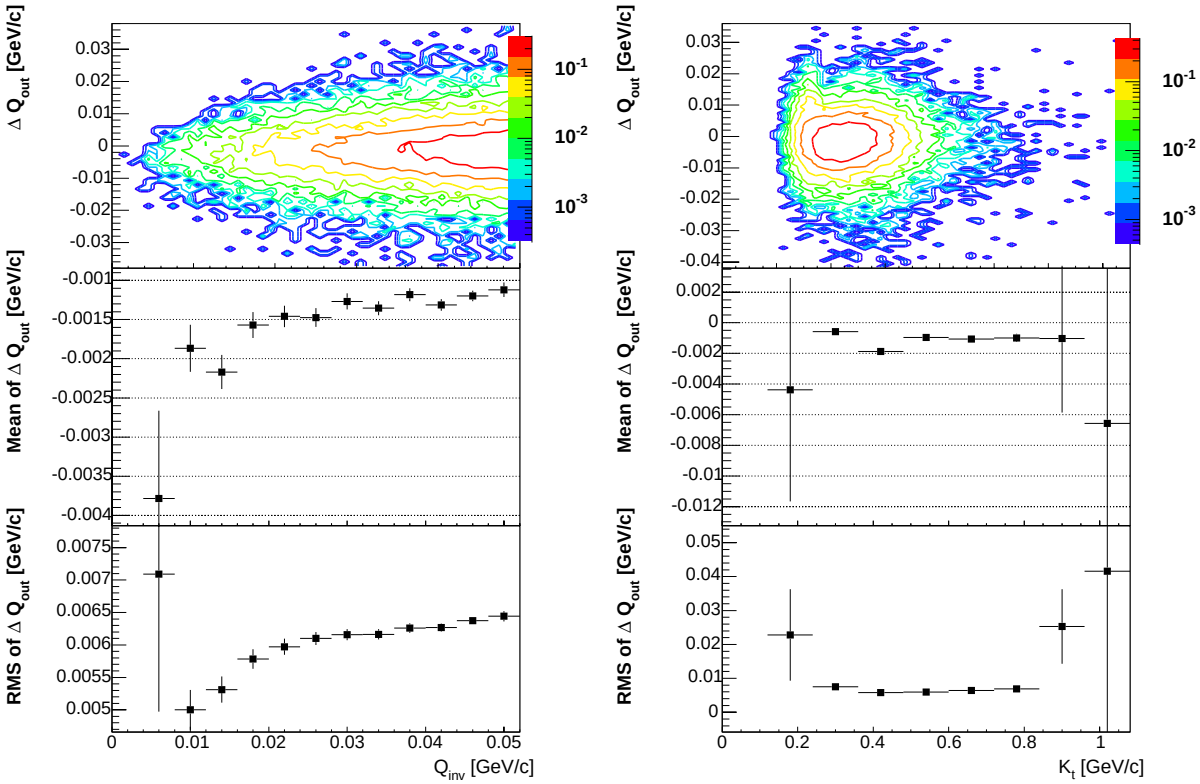

(a) (b)

Figure 30: Q_{out} resolution versus Q_{inv} (a) and K_t (b) for K^+K^+ system

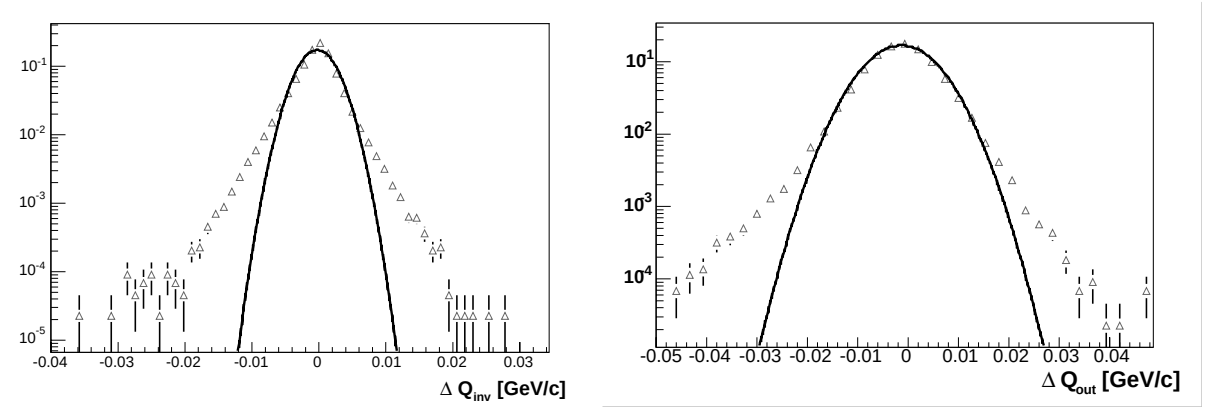

(a) (b)

Figure 31: Integrated residuals for Q_{inv} (a) and Q_{out} (b) for K^+K^+ system

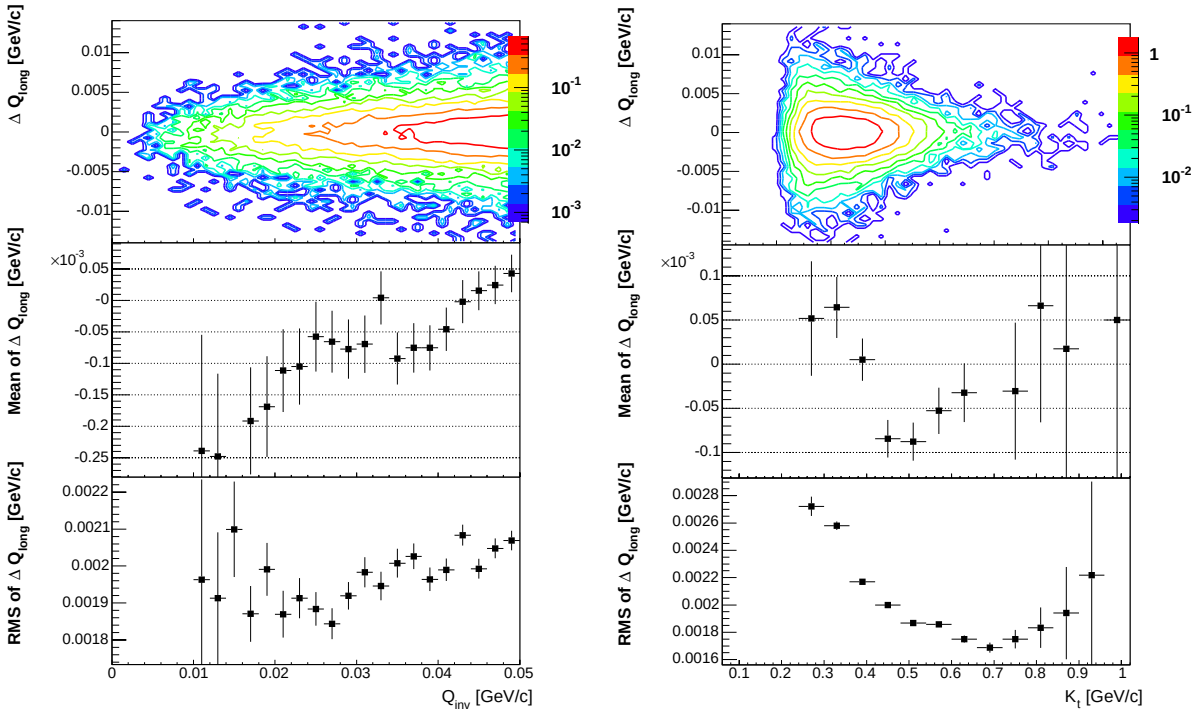

(a) (b)

Figure 32: Q_{long} resolution versus Q_{inv} (a) and K_t (b) for K^+K^+ system

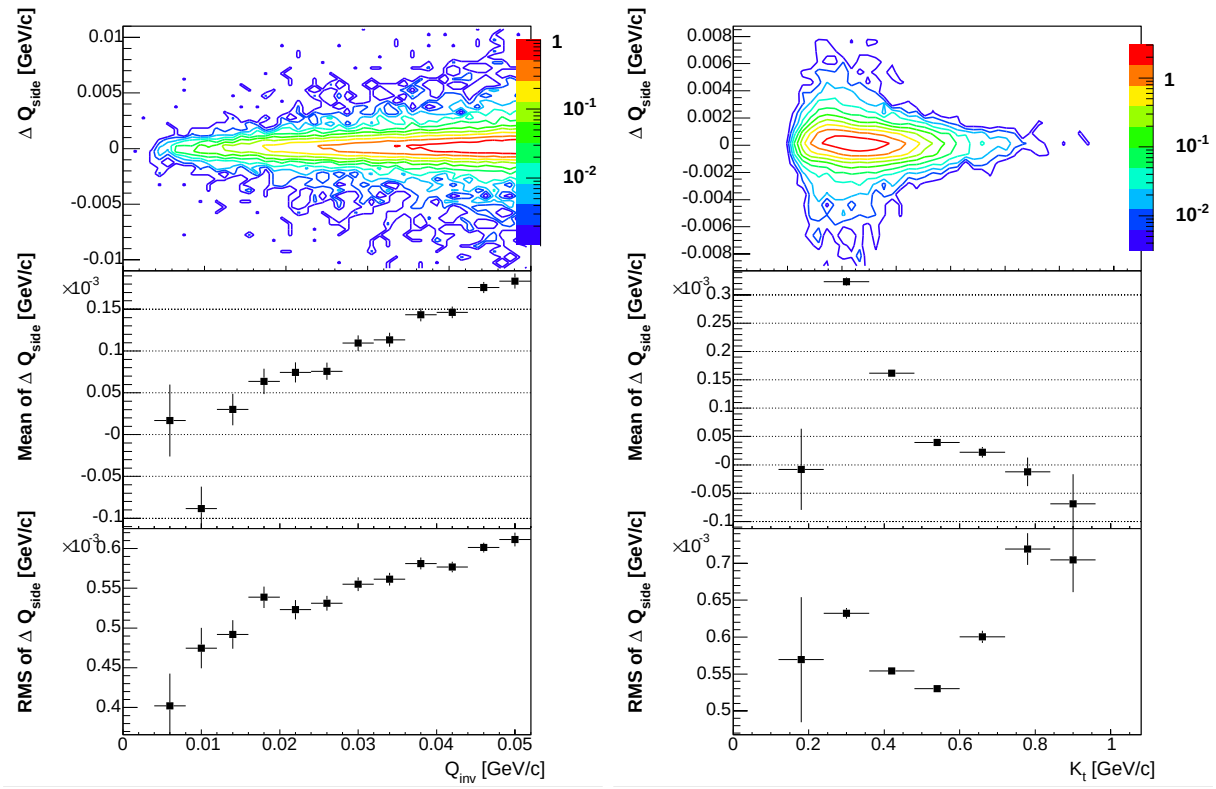

(a) (b)

Figure 33: Q_{side} resolution versus Q_{inv} (a) and K_t (b) for K^+K^+ system

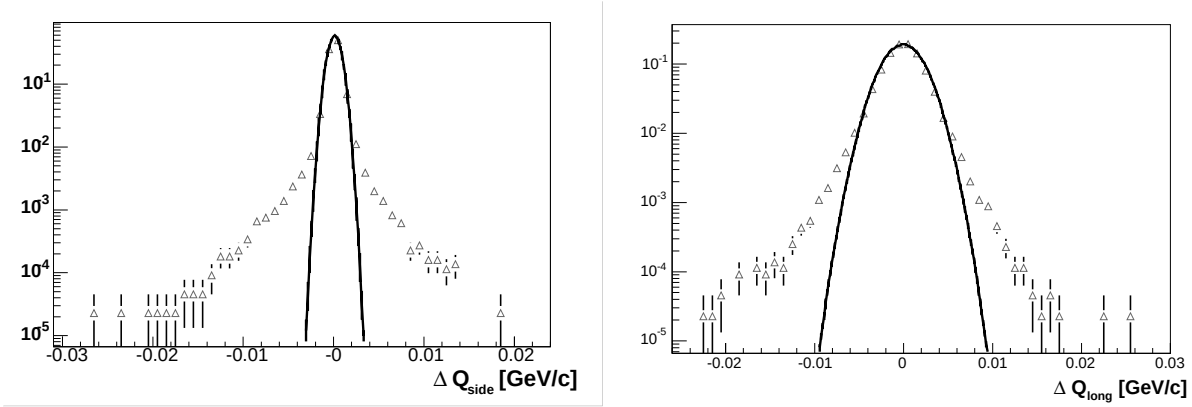

(a) (b)

Figure 34: Integrated residuals for Q_{side} (a) and Q_{long} (b) for K^+K^+ system

B.1.3 *pp*

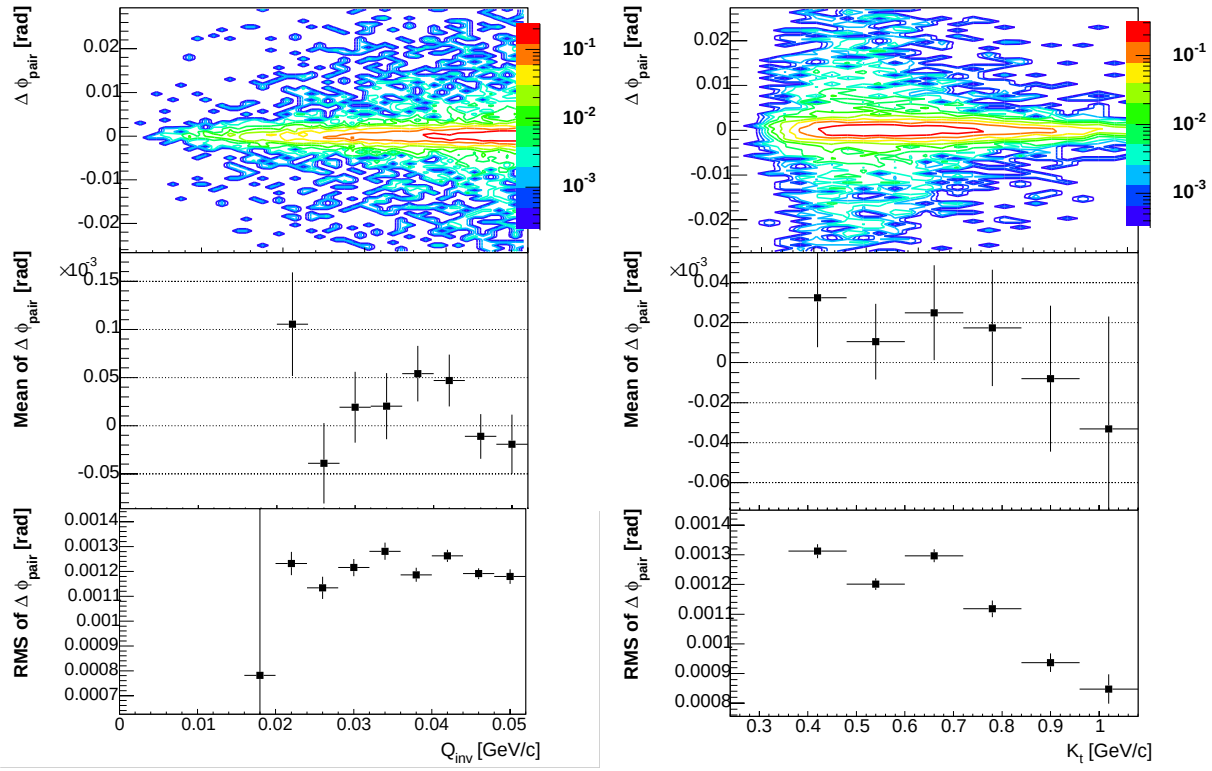

(a) (b)

Figure 35: ϕ_{pair} resolution versus Q_{inv} (a) and K_T (b) for $proton - proton$ system.

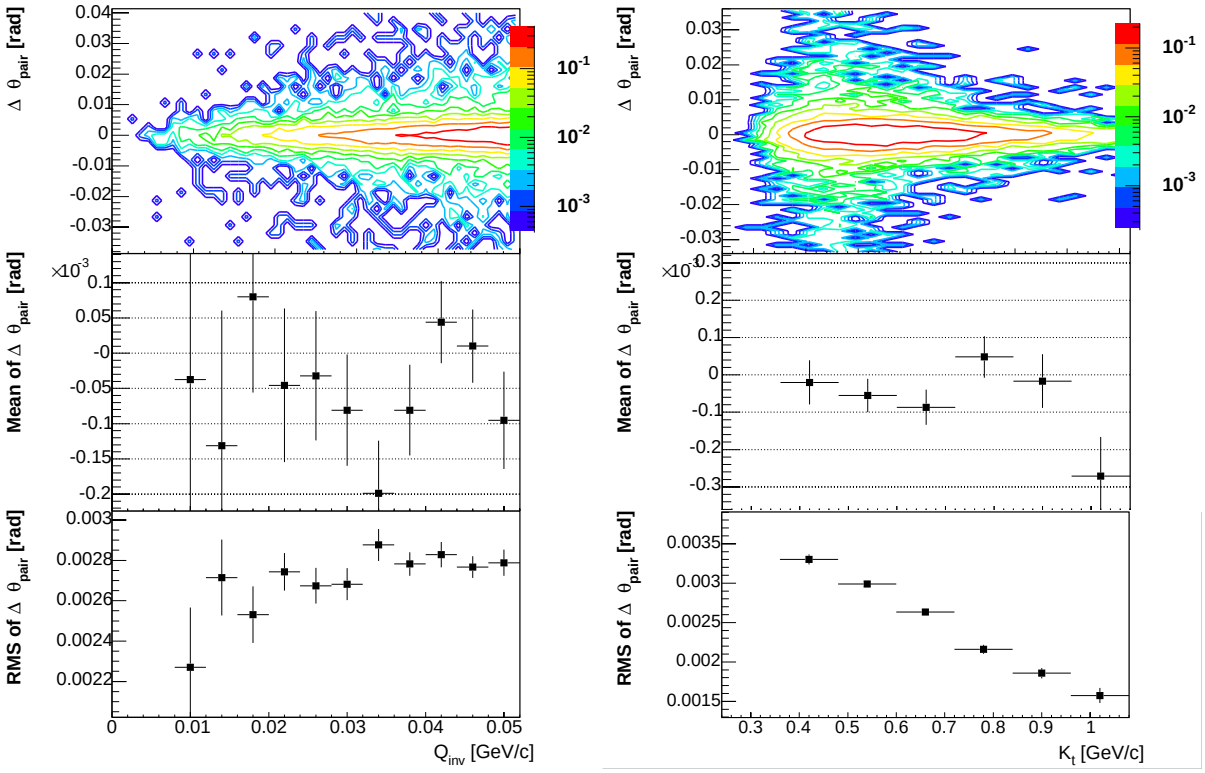

(a) (b)

Figure 36: θ_{pair} resolution versus Q_{inv} (a) and K_T (b) for $proton - proton$ system

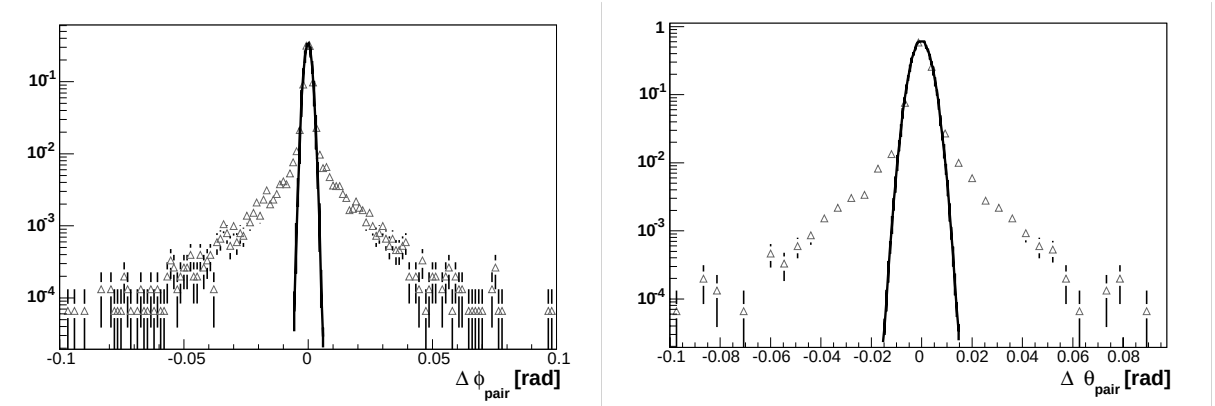

(a) (b)

Figure 37: Integrated residuals for ϕ_{pair} (a) and θ_{pair} (b) for $proton - proton$ system

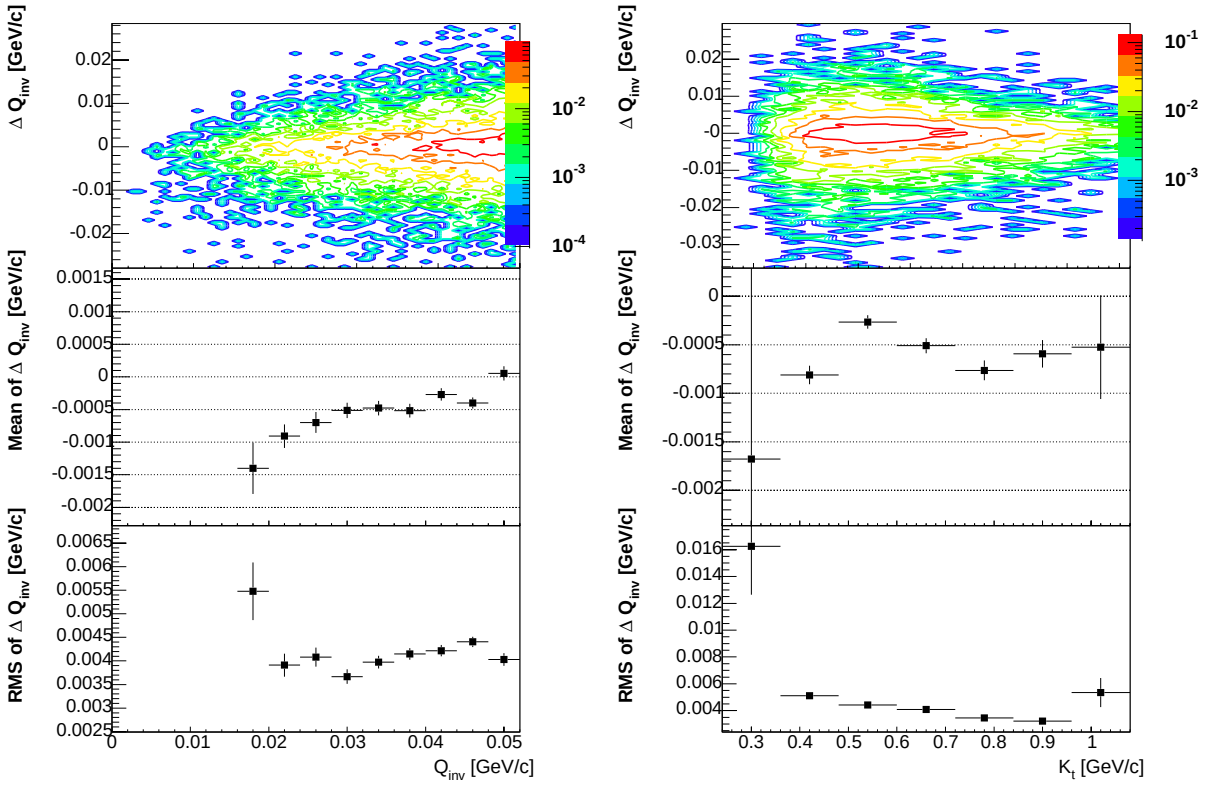

(a) (b)

Figure 38: Q_{inv} resolution versus Q_{inv} (a) and K_T for $proton - proton$ system

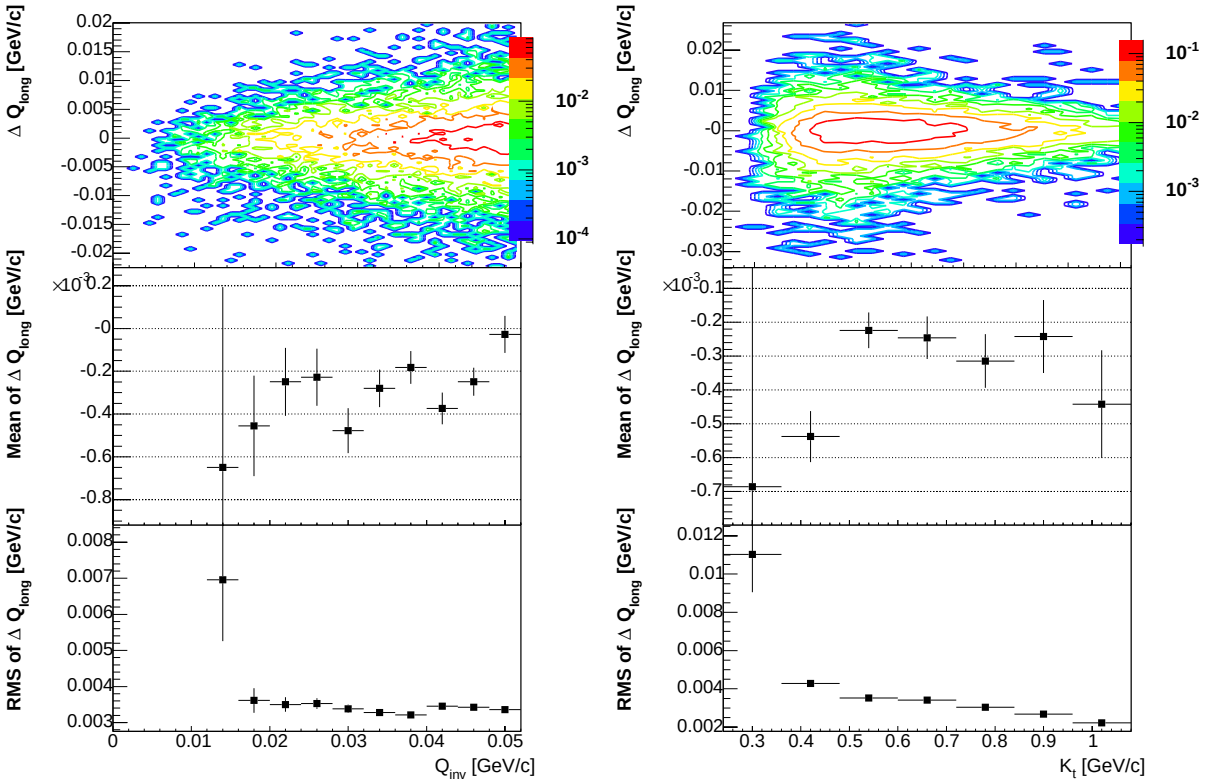

(a) (b)

Figure 39: Q_{long} resolution versus Q_{inv} (a) and K_T (b) for $proton - proton$ system

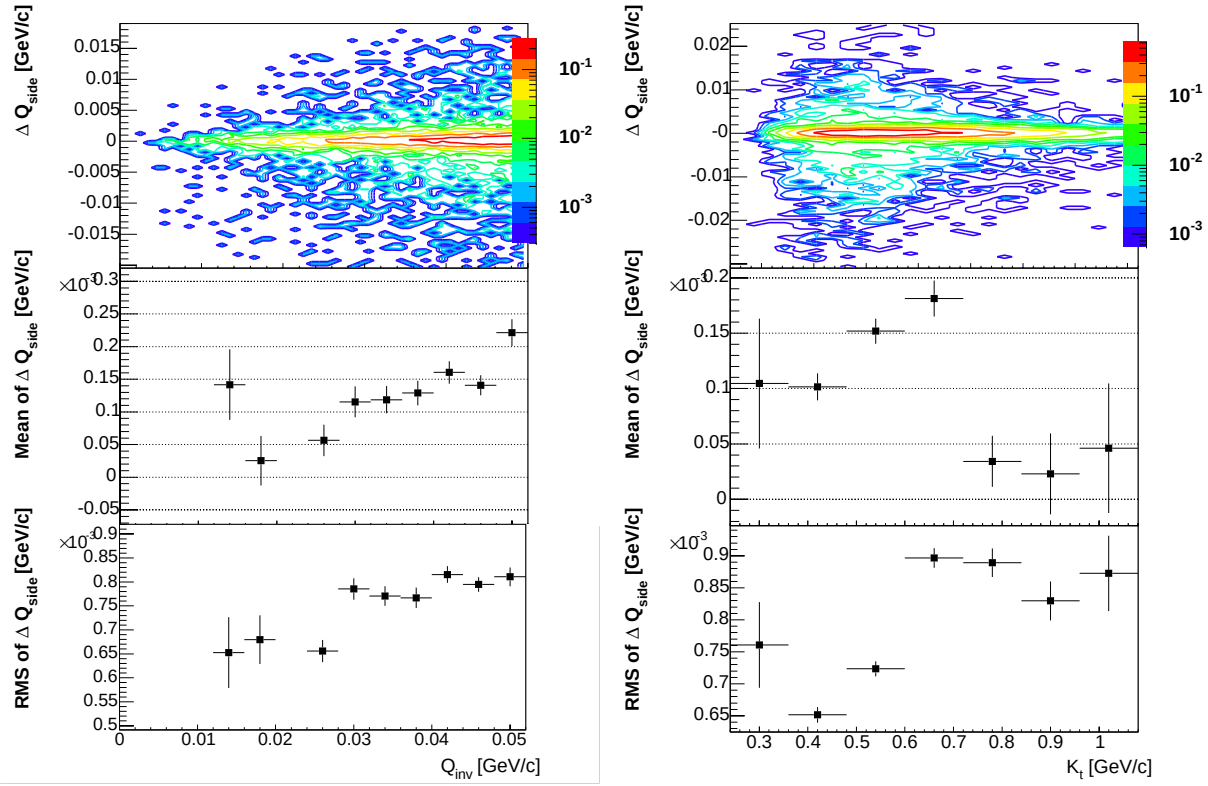

(a) (b)

Figure 40: Q_{side} resolution versus Q_{inv} (a) and K_T (b) for $proton - proton$ system

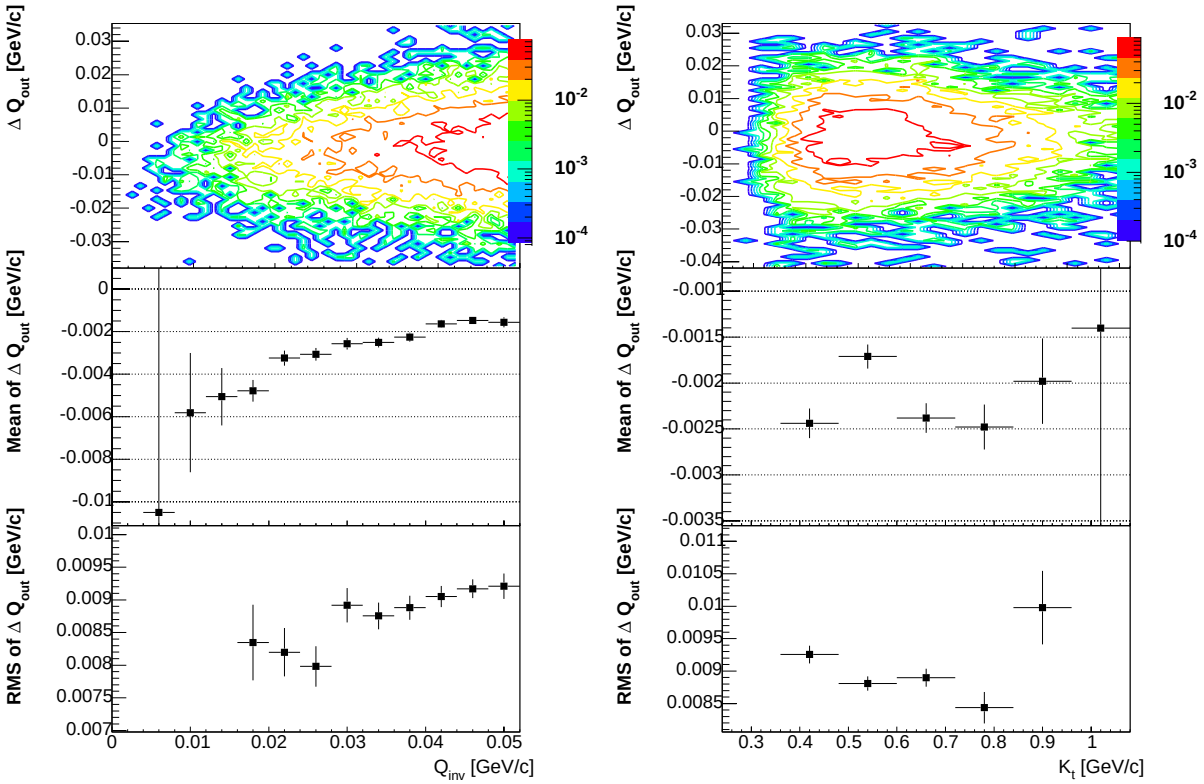

(a) (b)

Figure 41: Q_{out} resolution versus Q_{inv} (a) and K_T (b) for $proton - proton$ system

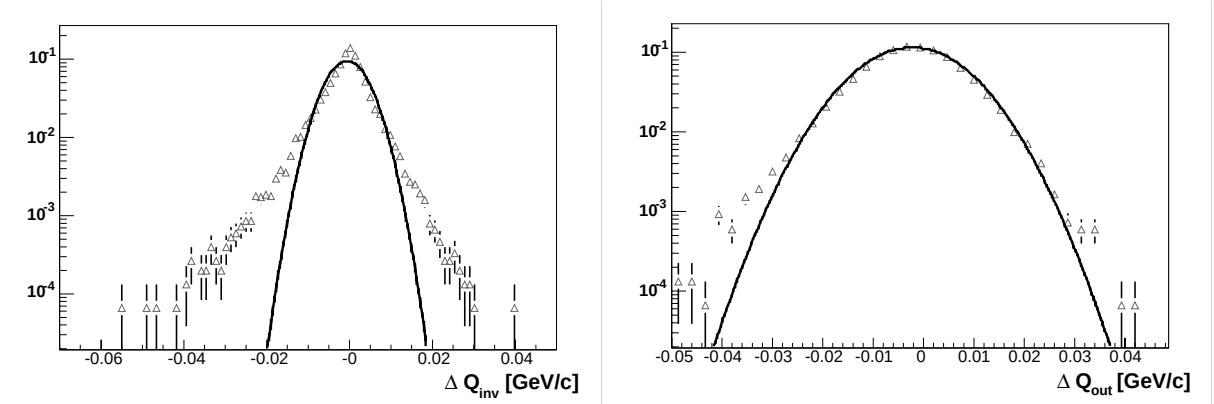

(a) (b)

Figure 42: Integrated residuals for Q_{inv} (a) and Q_{out} (b) for $proton - proton$ system

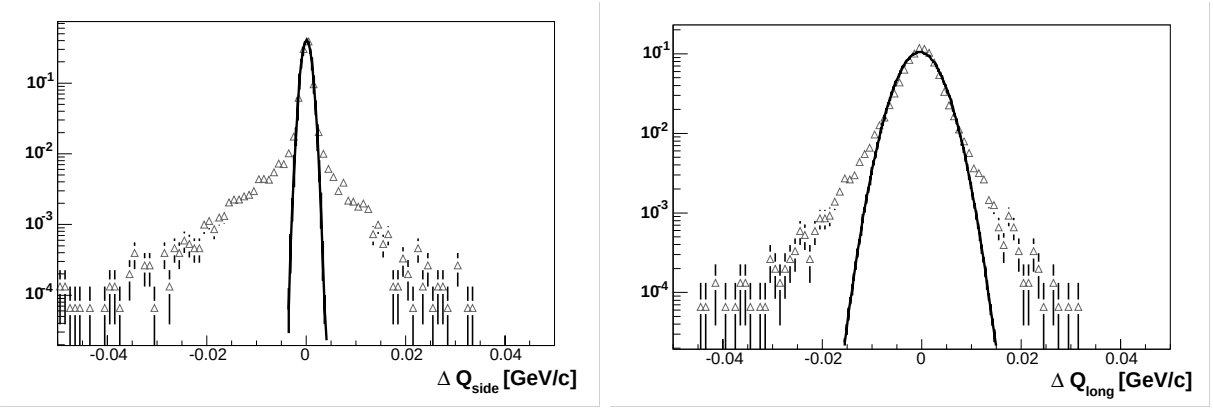

(a) (b)

Figure 43: Integrated residuals for Q_{side} (a) and Q_{long} (b) for $proton - proton$ system

B.2 Non-identical

B.2.1 $\pi^+\pi^-$

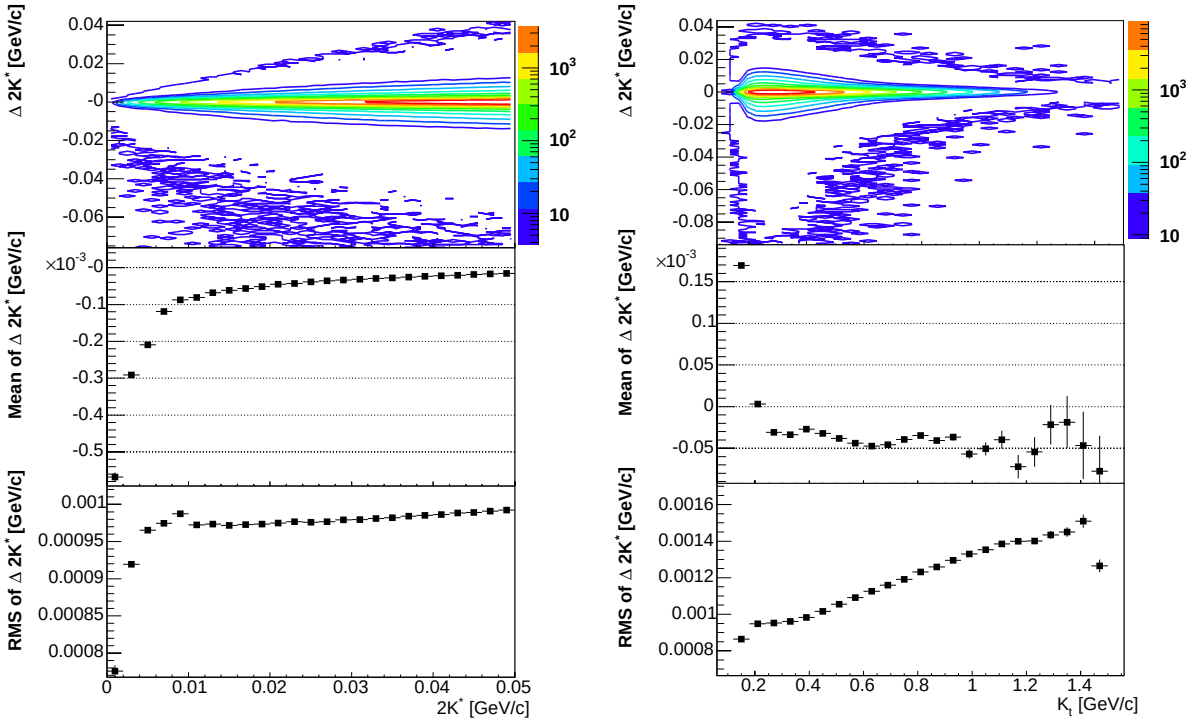

(a) (b)

Figure 44: $\pi^+\pi^-$ resolution versus a) $2 * k^*$ and b) K_t.

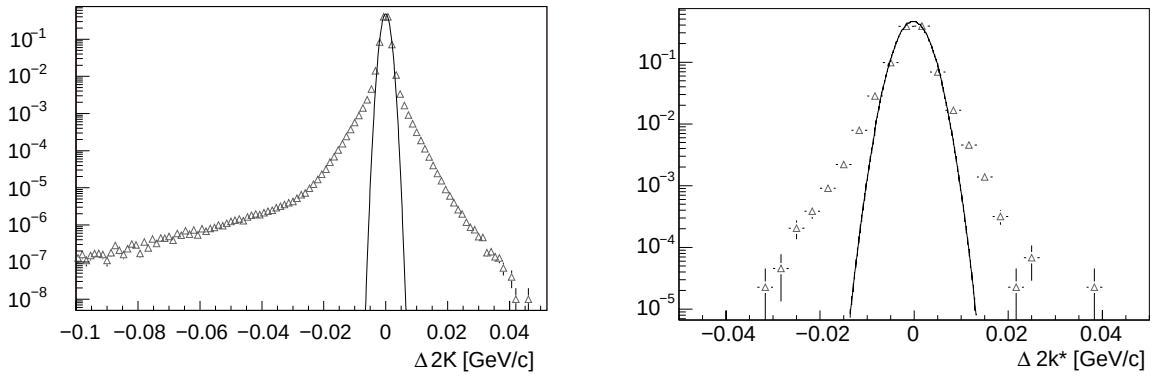

(a) (b)

Figure 45: $2 * k^*$ residuals for a) $\pi^+\pi^-$ and b) K^+K^-.

B.2.2 K^+K^-

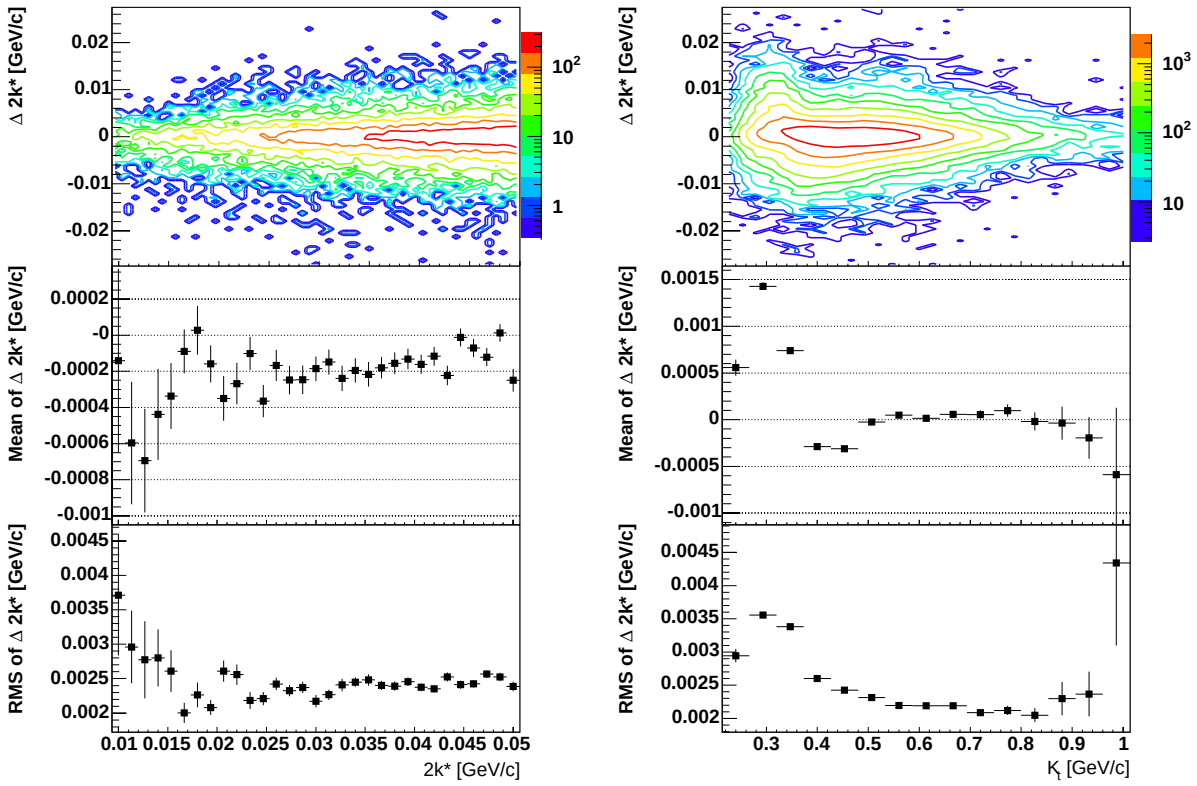

(a) (b)

Figure 46: K^+K^- resolution versus $2k^*$ (a) and K_t (b)

B.2.3 πK

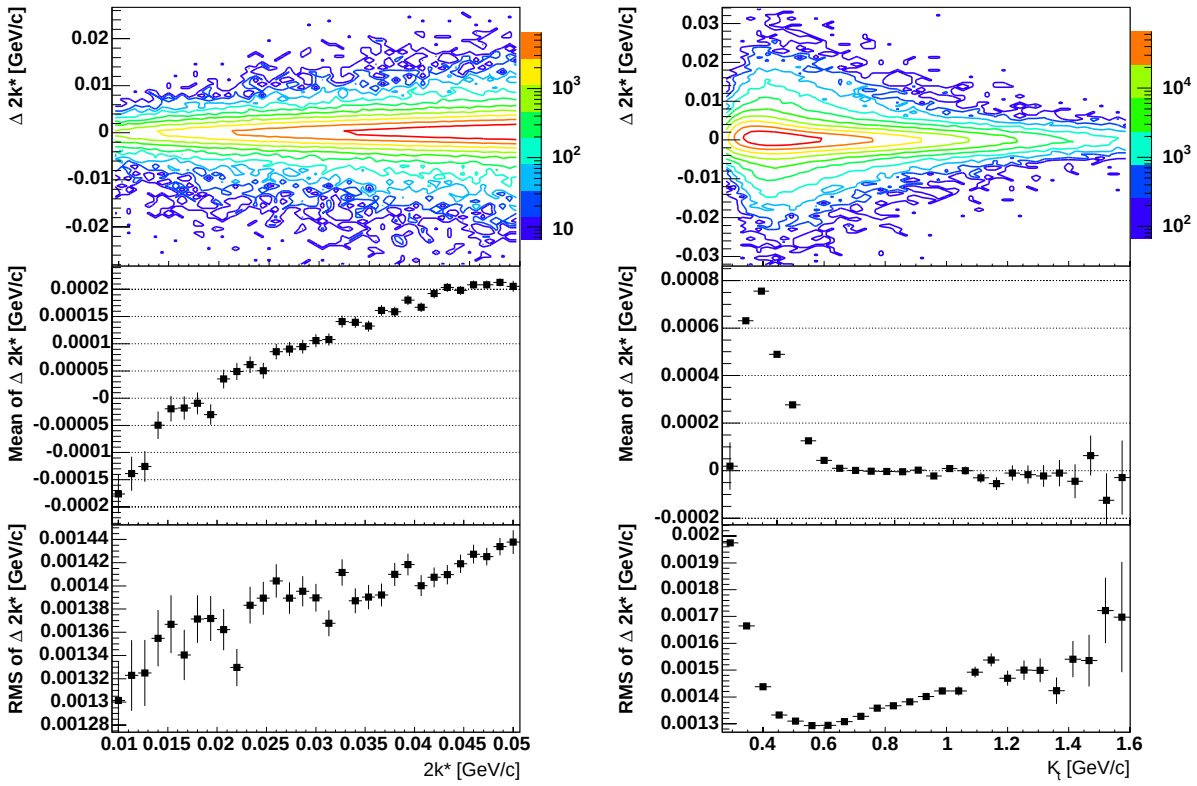

(a) (b)

Figure 47: π^+ - K^+ resolution versus $2k^*$ (a) and K_t (b)

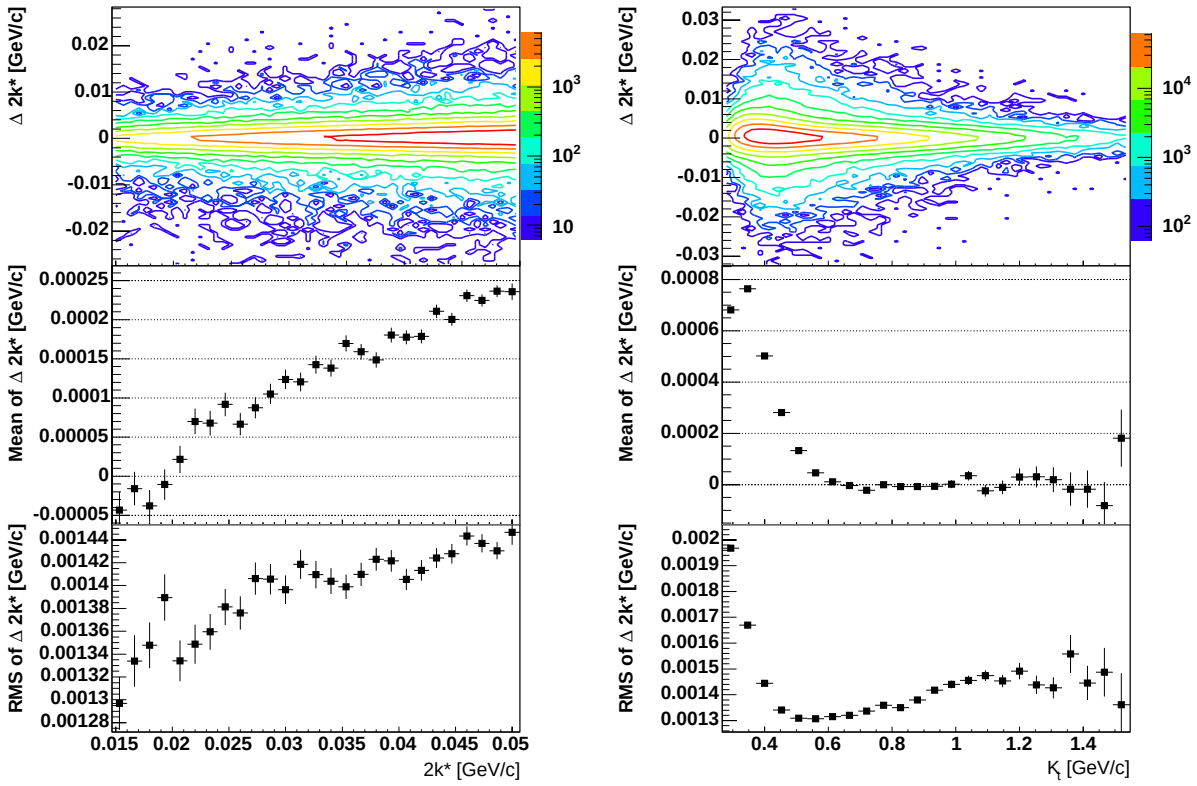

(a) (b)

Figure 48: π^+ - K^- resolution versus $2k^*$ (a) and K_t (b)

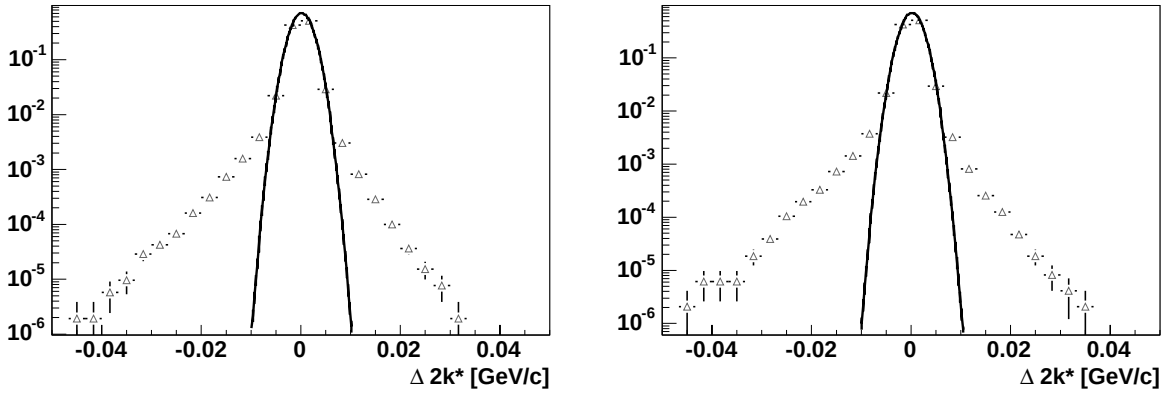

(a) (b)

Figure 49: Integrated residuals for π^+ K^+ (a) and π^+ K^- (b) systems

B.2.4 πp

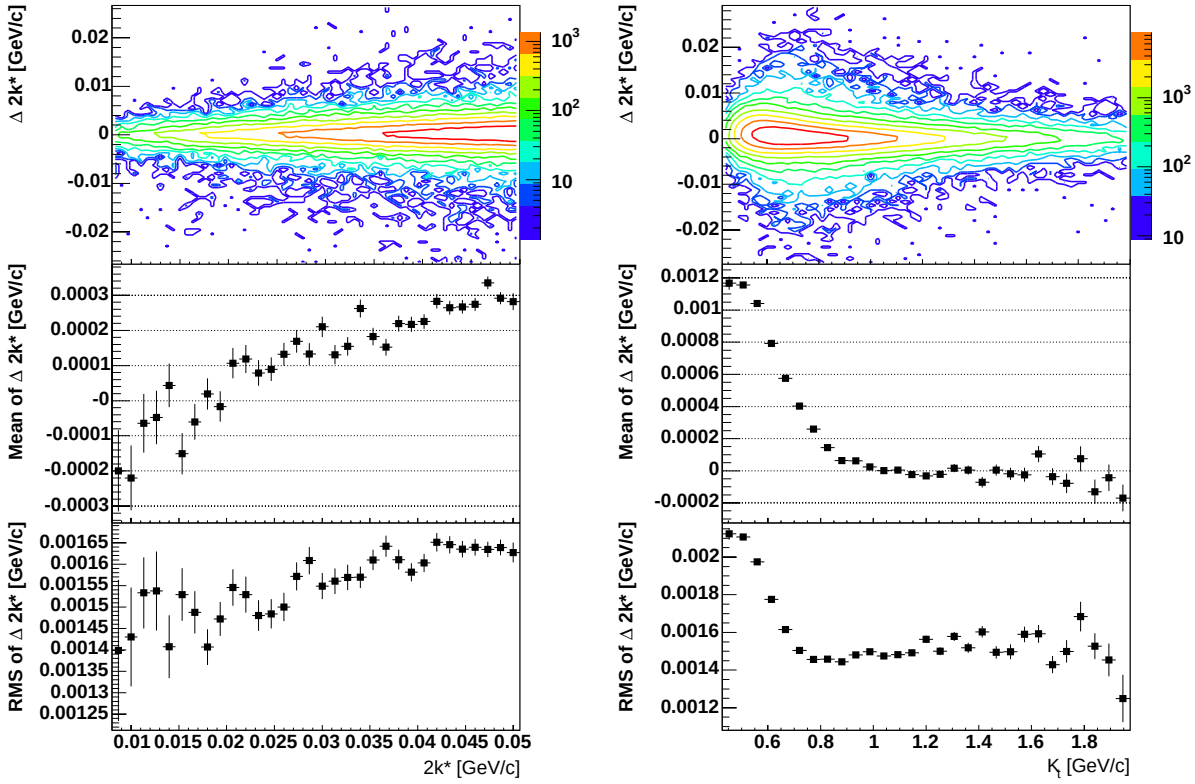

(a) (b)

Figure 50: π^+p resolution versus $2k^*$ (a) and K_t (b)

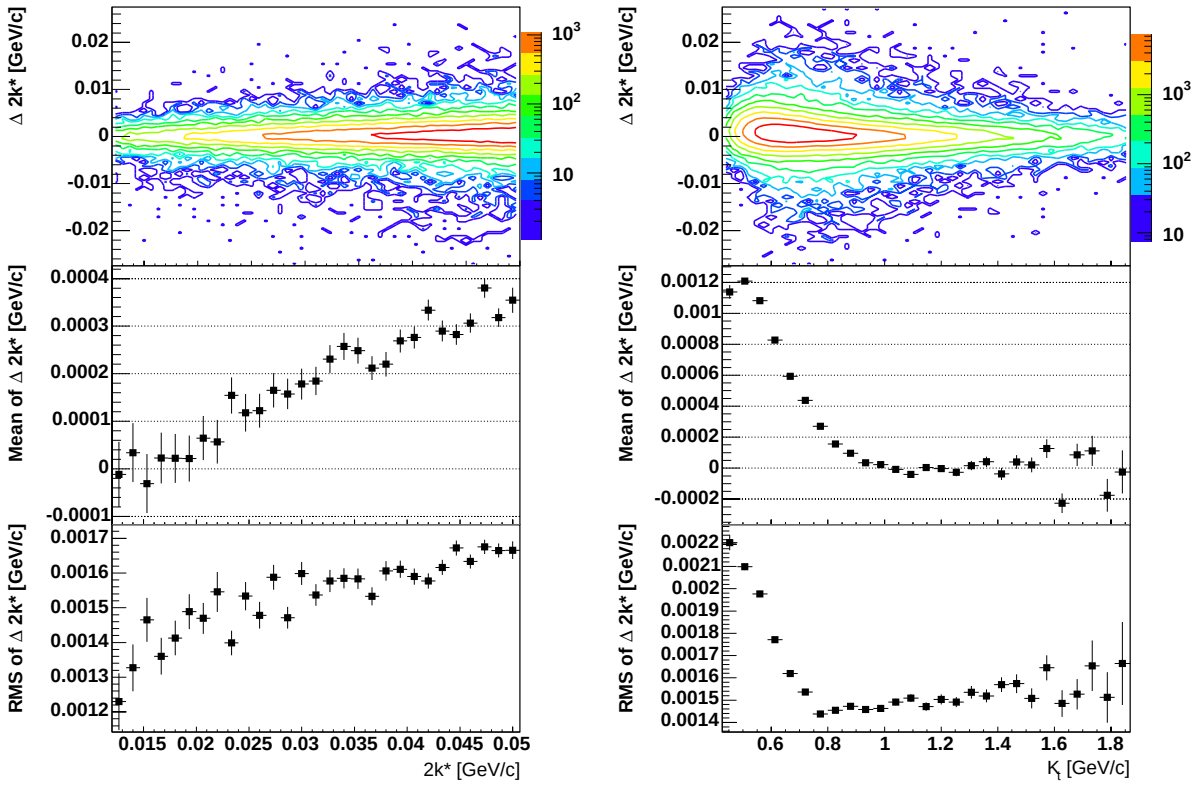

(a) (b)

Figure 51: $\pi^+\bar{p}$ resolution versus $2k^*$ (a) and K_t (b)

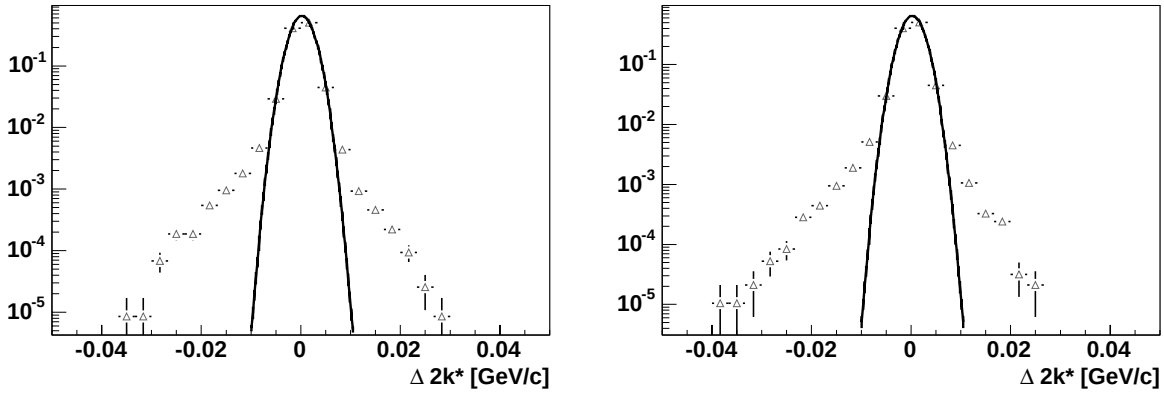

(a) (b)

Figure 52: Integrated residuals for π^+p (a) and $\pi^+\bar{p}$ (b) systems

B.2.5 Kp

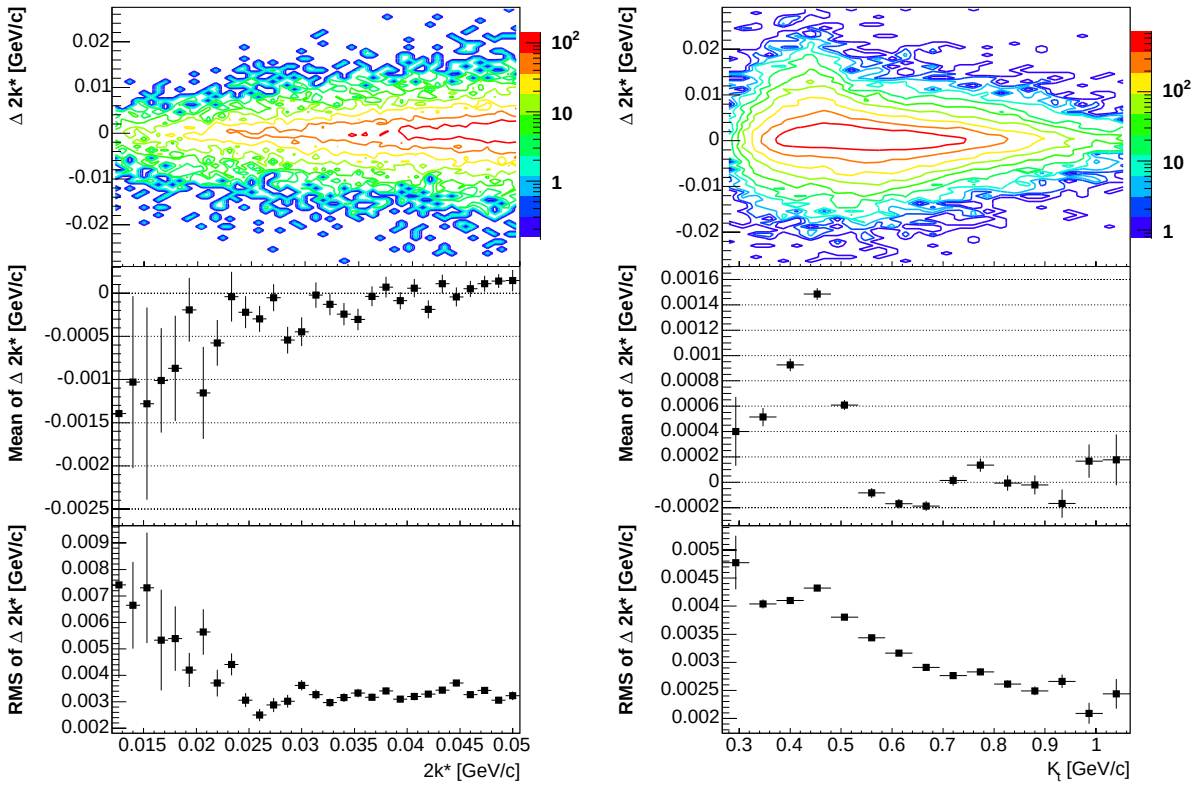

(a) (b)

Figure 53: K^+p resolution versus a) $2k^*$ and b) K_t

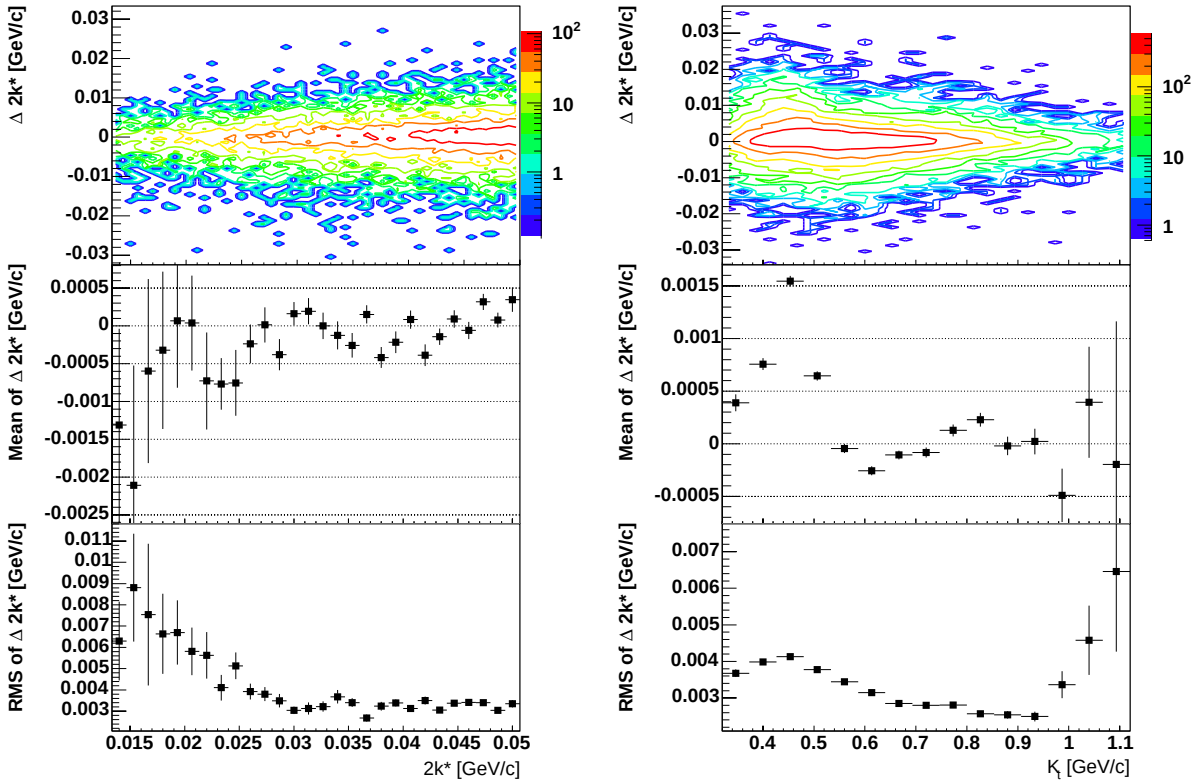

(a) (b)

Figure 54: $K^+\bar{p}$ resolution versus (a) $2k^*$ (b) and K_t

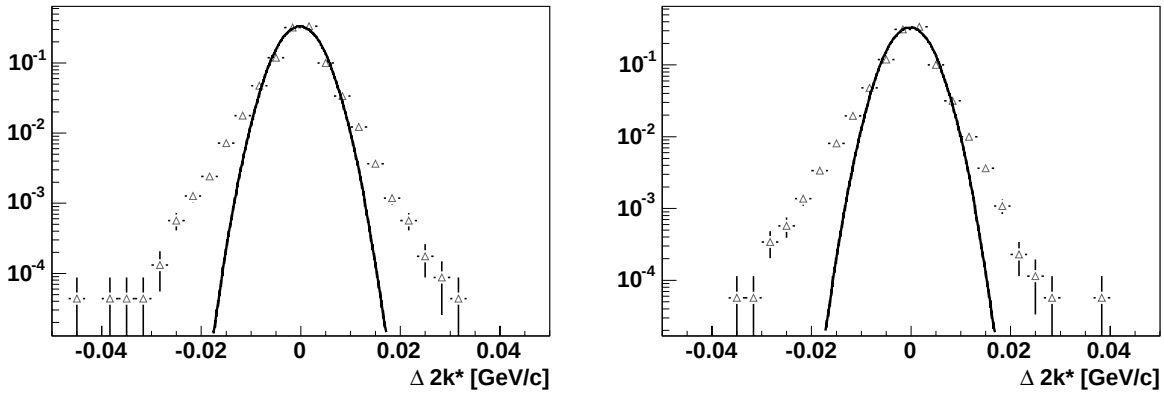

(a) (b)

Figure 55: Integrated residuals for (a) K^+p and (b) $K^+\bar{p}$ systems

References

[1] ALICE Collaboration, Computing Technical Design Report

[2] ALICE Collaboration, Alice Technical Proposal, LHCC-95 (1995)

[3] http://aliweb.cern.ch/people/skowron/results/PDC04/cent1/index.html

[4] http://aliweb.cern.ch/people/skowron/results/PDC04/cent1/CutStudy/res.single.pi+pi+.html